Satakunnan ammattikorkeakoulu
Satakunta University of Applied Sciences

FADDOUL, YVES MARIE

Design and Development of a Lab-Scale Filament Shredder for Additive Manufacturing Waste Recycling

DEGREE PROGRAMME IN MECHATRONICS
2025

ABSTRACT

Faddoul, Yves Marie: Design and Development of a Lab-Scale Filament Shredder for Additive Manufacturing Waste Recycling
Bachelor's thesis
Mechatronics
May 2025
Number of pages: 75

The automation laboratory at Satakunta University of Applied Sciences generates a steady stream of polylactic-acid (PLA) waste originating from failed prints, support structures, and filament changes. At present, these residues are discarded, contradicting institutional sustainability goals and losing material value. The objective of this thesis was therefore to design, fabricate, and evaluate a compact, maintainable shredder capable of converting laboratory PLA waste into uniform flakes suitable for re-extrusion.
The work was composed of four stages: (1) requirement definition from literature and laboratory interviews; (2) detailed computer-aided modelling in SolidWorks; (3) procurement and in-house fabrication of custom parts; and (4) a planned test program. Key design features include a single-shaft cutter stack with printed PETG spacers for rapid clearance adjustments, a modular mild-steel frame built from mitre-cut box tubing, and a low-cost control scheme centered on an ESP32 microcontroller and a recycled laboratory VFD.
Fabrication progressed to full plasma-cutting and deburring of all panels, blades and spacers, and welding of the base frame rectangle. Tool failures and material supply errors, namely an initial batch of stainless tubing that dulled saw blades and a 10 mm plate received in place of an intended 6 mm plate, consumed the build window, leaving the upper-frame welding, wiring, and motor integration outstanding. As a result, no powered trials could be conducted within the thesis schedule. However, hand-rotation checks confirmed concentric alignment of the blade-spacer stack, and redesigns completed during the delay (button box mount, reinforced electronics enclosure, and the addition of PETG-printed spacers for alignment control) position the prototype for rapid completion.
The project delivers a validated CAD package, complete cut parts, and a partially assembled frame, demonstrating the feasibility of an in-house, maintainable shredder tailored to AM waste. Immediate work should finish welding, install the drivetrain, and execute the planned no-load, light-load, and emergency stop tests. Once commissioned, the machine is expected to divert a significant amount of filament waste every year from the landfill and provided a closed-loop teaching platform for sustainable manufacturing practices.

Keywords: PLA waste, laboratory shredder, circular economy, additive manufacturing

CONTENTS

1 INTRODUCTION

1.1 Background and Motivation

Additive manufacturing, better known as 3D printing, has become widespread in educational and industrial settings due to its general ease of use and ability to manufacture small, cost-effective parts. The global 3D printing industry expanded to a value of 11.967 billion dollars in 2019, reflecting a growth rate of 29.9% (Zhu et al., 2021). According to Zhu et al. (2021), "*3D printing has tremendous advantages such as fast design and production, cost-effectiveness, ease of access, rapid prototyping, flexible designing, reducing waste, and being environment friendly.*" These advantages, compared to traditional manufacturing methods, have resulted in a sharp rise of utilization of the technology, including in sectors such as healthcare products, dental materials, toys, aviation, and others, with research suggesting further potential in numerous fields. However, this growth has also resulted in a rise in plastic waste associated with 3D printing. Waste is commonly generated through failed prints, post-processing support material removal, and more recently, filament-swapping techniques, where filament feedstock is exchanged mid-print for another type or color. Zhu et al. (2021) estimate that 3D printing filament waste could have generated at least 5000 tons of unused materials in 2020. This volume may further increase proportionally as additive manufacturing adoption expands.
Among 3D printing materials, polylactic acid (PLA) is one of the most widely used and significant sources of 3D printing waste. Due to its relative durability, low cost, and excellent printability, PLA has quickly become a staple in additive manufacturing, holding a large share of the filament market.

1.2 Problem Definition

Currently, the Satakunta University of Applied Sciences' laboratories make extensive use of 3D printers, with PLA being by far the most commonly used filament. However, despite its high usage, the university does not currently employ any efficient method for recycling PLA waste. Instead, filament waste is often disposed of, which not only contradicts sustainability and circular economy goal but also results in opportunity costs associated with the disposal of potentially reusable material. Despite the significant economic and environmental benefits of recycling filament waste, most commercially available shredders are either too large and intended for industrial applications, too expensive, or unsuitable for educational environments due to safety concerns, maintenance complexity, and lack of scalability for small-batch applications.

1.3 Objectives

The objective of this thesis is to design, model, prototype, and test a laboratory-scale shredder for PLA recycling that supports circular economy principles. The shredder must be suitable for laboratory use where operators include university staff and students.

The design must prioritize high maintainability to ensure that long-term wear and tear can be addressed easily. Replacement parts should be simple to manufacture or procure, and critical components must be accessible for servicing. In addition, the shredder must operate efficiently, processing significant volumes of filament waste generated by the laboratories without requiring excessive manual intervention or downtime.

Finally, the shredder must be suitable for continued recycling cycles, including re-extrusion into new filament, thus closing the material loop within the laboratory ecosystem and full adhering to circular-economy principles.

1.4 Scope and Limitations

The scope of this thesis includes the design, modelling, prototyping, and testing of a laboratory-scale filament shredder for PLA waste recycling. It covers component selection, CAD modelling, the integration of safety measures, and a sustainability evaluation to ensure alignment with circular economy principles. In addition, a review of existing plastic shredding technologies, sensor applications, and circular economy frameworks relevant to filament recycling is conducted to support the design decisions.

The thesis does not cover full re-extrusion system development, industrial or commercial certifications, mass production, or long-term durability testing beyond initial trials.

1.5 Thesis Structure

Chapter 2 presents the literature review, providing background information on plastic shredding technologies, sensor systems, material recycling processes, and circular economy principles.

Chapter 3 defines the Requirements and Functional Specifications, establishing the functional and non-functional goals that guided the design of the filament shredder.

Chapter 4 describes the Conceptual Design process, including comparisons of design options and the reasoning behand the selected design architecture.

Chapter 5 covers Component Selection and Material Choices, detailing the selection of blades, shafts, motors, sensors, and other critical elements.

Chapter 6 presents the Detailed Design and Modelling, including CAD modelling, mechanical integration, and design refinements based on operational needs.

Chapter 7 discusses the Build Process and In-Lab Manufacturing efforts, documenting the physical prototype.

Chapter 8 describes Testing and Results, evaluating the design performance and identifying operational characteristics.

Chapter 9 provides the Discussion, reflecting on the success of the design against the initial requirements and considering sustainability impacts.

Chapter 10 concludes the thesis by summarizing key findings and suggesting directions for future work.
References and Appendices provide supporting material, including cited literature, technical datasheets, and detailed calculations.

2 LITERATURE REVIEW

2.1 Introduction

This chapter reviews the current state of affairs in small-scale plastic shredding systems, covering mechanical designs, power and energy requirements, safety measures, sensing and control strategies, performance metrics, and sustainability considerations. Information is gathered exclusively through recent peer-reviewed studies of PLA/PETG shredders, sensor application notes, circular-economy and life-cycle analyses (LCA), and EU policy documents to provide a foundation for the design of a university-lab filament crusher.

2.2 Shredding Mechanisms

Shredders convert waste plastics into smaller particles via rotating blades and shafts. The most common shredder configurations in small-scale systems are single-shaft, dual-shaft, and rotor-stator designs In single-shaft shredders, a single rotating shaft pulls the material against a fixed counter-blade, producing relatively uniform flakes. Dual-shaft shredders use two counter-rotating shafts that grab and shear material between them, offering greater torque and shredding power and are often used for tougher materials. Rotor-stator systems combine a rotating element (rotor) and a fixed surface (stator) to achieve precise cutting and grinding action.
The basic layouts of these shredder types are shown in Figure 1.

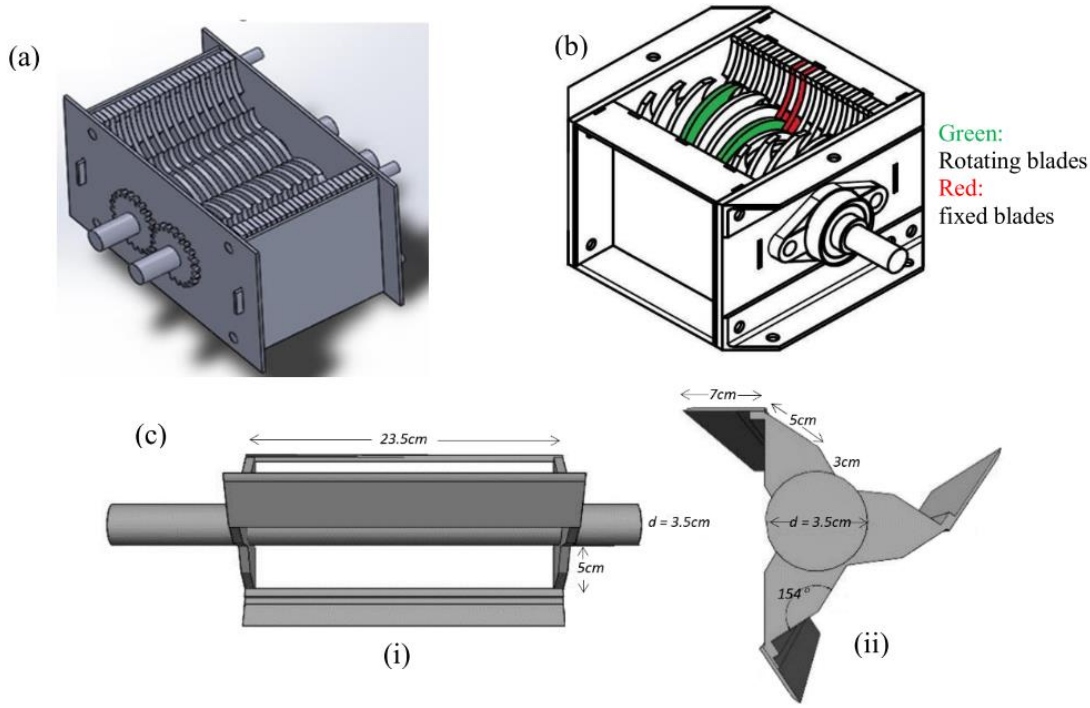

Figure 1 ***Shredder configurations:*** *(a) Double shafts, (b) Single shaft, (c) Single shaft with horizontal blade (i) side view and (ii) front view.*

Reprinted from Wong et al. (2022)

Building on these basic blade geometries, blade design becomes critical for performance. "[A shredder] uses specially designed rotating blade technology to produce high-precision plastic flakes" (Harjuma et al., 2024, p. 77), underscoring the importance of blade geometry for consistent particle size. Wong et al. (2022) survey shredder geometries, demonstrating that blade-orientation angles and inter-blade spacing critically influence particle-size distribution, with smaller clearances producing finer flakes. Specifically, "the geometry and orientation of the blades that were fitted into the single or double-shafts were found to directly affect the shredding performance" (Wong et al., 2022. p. 1).

2.3 Power and Energy Requirements

Motor sizing and specific energy consumption are critically important in shredder efficiency. Landolfi et al. (2024) employ a Design of Experiments (DoE) approach to optimize the recycling process of PET, achieving a 30% reduction in overall energy consumption through parameter optimization. As they conclude, "by optimizing printing parameters, energy consumption can be reduced

by up to 30%, while the tensile strength of the printed samples can be increased by 20%," (Landolfi et al., 2024, p.1), indicating that process tuning yields significant savings.

2.4 Safety Features

Lab-scale shredders benefit in safety metrics by including safety measures such as interlocked feed hoppers, blade guards, and emergency-stop circuits. Harjuma et al. (2024) emphasize that the plastic shredder must be designed with operator safety in mind, equipping it with adequate protection features to prevent accidents and facilitate simple, safe maintenance.

2.5 Sensing and Control

Detecting feed presence, overloads, and output flow is essential for automated safety and efficiency. Time-of-Flight (ToF) laser sensors offer rapid, contactless detection. The TMF880X family provides high-resolution distance and motion data up to 10 m, enabling detection of feed jams and static obstructions via median filtering and low-pass velocity thresholds (ams-OSRAM, 2025). In their application note, ams-OSRAM (2025) states that the ToF approach provides “high-resolution, real-time data on object proximity and position." (p. 1) By leveraging the ToF approach, the crusher would be prompted to stop immediately upon blockage detection. Programmable light-curtain systems extend this concept: they measure the presence of objects intersecting user-defined curtain surfaces and produce data at significantly higher resolution than LiDAR in their region of focus (Ancha et al., 2022, pp. 1-2). Such systems remain largely experimental.

2.6 Performance Metrics and Evaluation

Key metrics include throughput (kg/h), particle-size distribution (D10-D90), energy per mass shredded, blade-wear rate (hours/blade), and noise/vibration levels. Throughput directly impacts how efficiently filament waste can be

processed during high-usage periods, while a consistent particle-size distribution is critical for successful re-extrusion into new filament. Particle-size distribution is typically described using D10-D90 values, indicating the size range within which 80% of particles fall. A narrow D10-D90 range ensures more predictable melting and extrusion behaviour during filament processing. Low energy consumption is essential to minimize operational costs and environmental footprints, aligning with university sustainability goals. High blade-wear rates increase maintenance demands and operating costs, reducing the system's viability for long-term lab use. Finally, managing noise and vibration levels is important for ensuring safe and comfortable operation within shared educational environments.

In order to effectively recycle and reuse filament waste, the waste must first be shredded and reduced to small flake sizes. In general, the smaller the average flake is in a batch of shredded filament waste, the higher the quality of recycled filament is. Hasan et al. (2024) suggest that the "appropriate size [of filament flakes] should be within the range of 5 mm", and that "if shredded plastic particles are too large, they can lead to the inclusion of unmelted plastic particles in the extruded filament," (Hasan et al., 2024), reducing the material durability. A trade-off also exists between particles that are too small and the recycling process's duration, whereas the smaller the average particle is, the longer it takes to recycle it.

In addition to technical performance, environmental considerations play a critical role in evaluating the overall impact and sustainability of lab-scale shredding systems.

2.7 Environmental & Circular-Economy Considerations

Integrating shredders into closed-loop workflows aligns with EU circular-economy goals, which emphasize keeping materials in use and reducing raw resource extraction. The European Commission (2020) aims to promote sustainable products by enhancing durability, recyclability, energy efficiency, and overall circularity. Zhu et al. (2021) highlight the potential for recycling and reprocessing of 3D printed plastics such as PLA and PETG to contribute to

circular economy goals, though further specific quantitative life cycle assessments (LCAs) on CO_2 reduction are needed. An LCA quantifies the environmental impacts across all stages of a product's life, from raw material extraction to manufacturing, use, and product disposal. LCAs are essential for objectively comparing recycling strategies to traditional waste management methods and inform recycling and waste disposal decision-making processes. Hafiz et al. (2024) systematically review additive manufacturing (AM) recycling and highlight that research gaps remain in the economic feasibility of large-scale recycling processes, while contamination and sorting challenges continue to hinder recycled-content targets.

2.8 Recycling Workflows & Material Properties

Hasan et al. (2024) report that the mechanical recycling processes lead to a significant decrease in the molecular weight and tensile strength of recycled PLA (rPLA), with tensile-strength losses typically between 10% and 17%. Hasan et al. (2024) further emphasize the importance of moisture content control and thermal history in maintaining the mechanical properties and printability of recycled PLA. Multiple extrusion cycles in large-format systems yield modest degradation compared to desktop units, as moisture and thermal history are better controlled (Romani et al., 2024). Romani et al. find that "granulate recycled PLA feedstock processed with LFAM [Large-Format Additive Manufacturing] FGF [Fused Granular Fabrication] is less affected by thermomechanical degradation than desktop-size FFF [Fused Filament Fabrication] systems by avoiding further reprocessing steps on secondary raw materials, i.e., extruding filaments" (Romani et al., 2024, p. 11.), suggesting a workflow advantage for large-format granule extrusion. Hasan et al. (2024) discuss that strategies such as blending virgin and recycled PLA, adjusting extrusion temperatures, and using chain extenders can significantly improve the mechanical and thermal properties of recycled PLA, helping to mitigate degradation.

2.9 Gaps and Research Opportunities

Despite advances, gaps remain in sensor-integrated, low-cost feeders, full economic LCAs for lab-scale systems, and standard throughput benchmarks for mixed-polymer wastes. Contamination by colorants and composites poses challenges for consistent flake quality. Opportunities lie in combining ToF and light-curtain sensing for real-time jam detection, designs of blades and feed geometry for energy minimization, and embedding simple control logic into open-source hardware for broader adoption.

2.10 Summary

A review of PLA and PETG shredding literature reveals mature blade and shaft designs, considerations for motor energy efficiency, and well-established safety practices. Emerging research trends explore the integration of sensor technologies for machine monitoring and the adoption of circular economy frameworks supporting recycling and additive manufacturing.

The reviewed studies offer a strong foundation for the design of a laboratory-scale filament crusher. Key recommendations include selecting a single-shaft granulator architecture, using a motor appropriately sized for small-scale shredding tasks, implementing an interlocked or otherwise safeguarded enclosure, and considering Time-of-Flight (ToF) sensors for monitoring material feeding. Blade clearances should be tuned to produce flakes in the 2-5 mm size range, depending on desired output and sieving steps. Throughput expectations for small-scale systems are on the order of low single-digit kilograms per hour, consistent with laboratory and pilot-scale recycling setups.

Finally, alignment with European Union recycled-content targets and life-cycle assessments (LCA) best practices will enhance the relevance and sustainability of such designs.

3 REQUIREMENTS AND FUNCTIONAL SPECIFICATIONS

The functional and non-functional requirements for the laboratory filament shredder were determined based on preliminary research, discussions with the university laboratory, form responses, and sustainability objectives. These requirements guide the design, material selection, component choices, and safety features of the shredder.

3.1 Functional Requirements

- The shredder must be capable of processing only filament waste made of PLA.
- The shredder must handle printed parts with approximate maximum dimensions up to 200 mm x 200 mm.
- The shredder must shred PLA printed parts into flakes or particles suitable for re-extrusion into filament.
- The shredded material must be collected into a removable sliding bin accessible through an enclosure door.
- A slanted sieve must be installed underneath the shredder output to catch oversized flakes; these flakes must be guided into a secondary bin for manual reprocessing.
- The shredder must allow swapping full bins with empty ones without interrupting shredding operations for long periods.
- The shredder must operate continuously at a throughput appropriate for processing small batches (~500g to 1kg per session).
- The shredder must be manually operable via a physical start/stop interface for emergency or manual control override.
- The shredder must safely prevent user hand access into the cutting area either through the use of specially shaped feed chute that inhibits hand entry, or an interlock lid that acts as a safety switch that must be closed before startup operations.

- The shredder must include a manually operated emergency stop button (E-Stop) that immediately cuts power to the motor in case of emergency.
- The E-Stop button must be wired through a safety relay or equivalent fail-safe circuit to ensure immediate power isolation independently of software control.
- The shredder must shred printed PLA waste without requiring excessive pre-processing (i.e., minimal manual cutting of prints before feeding).

3.2 Non-Functional Requirements

- The shredder must be designed for safe operation in a shared university laboratory environment.
- The design must physically prevent hand access to the cutting mechanism through enclosure design, interlock lid, and/or chute geometry.
- The shredder must include a manually operated emergency stop (E-Stop) button wired through a safety relay or equivalent fail-safe mechanism to ensure immediate shutdown in case of emergency.
- The system should minimize operational noise through the use of an enclosed casing, but extremely low noise levels are not mandatory.
- The shredder footprint must be small enough to fit on a standard laboratory table or workbench, with approximate maximum dimensions of 500 mm x 500 mm x 500 mm (length x width x height).
- Maintenance operations, including blade replacement and bin emptying, must be simple and tool-assisted where necessary but not overly complicated.
- Component procurement must prioritize availability and cost-effectiveness, within the constraints of an educational institution budget.
- Sustainability must be considered by designing for durability, recyclability of materials used, and compatibility with circular economy goals.
- The machine must operate reliably for small-batch laboratory recycling without requiring frequent servicing or complex calibration.

4 CONCEPTUAL DESIGN

4.1 Overview of Design Requirements

As a brief reminder, the purpose of this filament shredder is to efficiently shred specifically PLA filament and must be suitable for a laboratory environment where operators are university students and staff. The size of the shredder must be desktop-sized with multiple safety features. Lastly, the shredder must be modular in its storage system, allowing the removal of the storage compartment and replacement to allow for continuous operation with minimal downtime. This section will detail and justify the design decisions made to fulfil these requirements.

4.2 Evaluation of Shredding Mechanisms

The shaft design of a shredder is one of its most important features; it dictates shredder efficiency, speed, and power. Multiple shaft styles exist, with the most suitable shaft styles for this project being a single-shaft system and a double-shaft system. (Wong et al., 2022, p. 3.)

A single-shaft system utilizes a set of rotating blades, powered by a motor. These rotating blades crush material against a set of stationary blades, resulting in the generation of uniform flakes. In double-shaft systems, the stationary blades are replaced with a second set of counter-rotating blades. Material is thus crushed between two counter-rotating blades, resulting in flake generation. (Wong et al., 2022, p. 3.)

According to Wong et al. (2022, p. 3), Double-shaft systems have increased shredding power and higher torque, resulting in greater capabilities in cutting action and cutting speed. Due to these advantages, they are ideal for handling tougher, larger, or rigid materials. However, their disadvantages lie in its increased cost and complexity. This results in longer manufacturing times, increased costs, greater wear and tear, and comparatively difficult maintenance. Conversely, single-shaft designs hold lower shredding power and torque and are less suitable for tougher materials. Despite these drawbacks, they boast a

simpler mechanical design, cheaper costs, and are easier to maintain. Furthermore, they excel at small-scale applications where the intention is to shred softer plastics in a laboratory environment where operators are not expected to be experts in shredder maintenance protocols.
Since PLA is a relatively brittle and easy-to-fracture material compared to engineering plastics like ABS or nylon, the shredding force required remains within the operational capabilities of a single-shaft system. This makes them ideal for this shredder project. Thus, the single-shaft design was selected for this project.

4.3 Blade Design and Arrangement

The blade system of the filament shredder is a critical subsystem that directly affects shredding efficiency, flake quality, operational reliability, and maintainability. In this section, key design choices for the blade geometry, arrangement, material, and maintenance strategies are detailed and justified. These decisions were made based on literature findings, mechanical reasoning, project constraints, and practical considerations relevant to a laboratory environment where the operators are students and staff.

4.3.1 Blade Geometry

Blade Diameter:
A blade diameter of 250 mm was selected to ensure sufficient cutting surface engagement and effective flake generation during shredding. This value defines the full tip-to-tip span of each blade, including the outer cutting edges, and indirectly influences both the cutting depth and mechanical leverage of the blades.

Number of Cutting Edges:
A two-edged blade design was selected. Research by Wong et al. (2022) indicates that increasing the number of cutting edges does not necessarily improve shredding performance and may increase material skipping and

jamming. Two-edged blades simplify manufacturing, reduce maintenance needs, and ensure robustness during operation.

Cutting Angle:

A cutting angle (Figure 2) of 70° was chosen. While literature does not conclusively link cutting angle to shredding performance, a larger angle provides a larger grabbing surface, aiding material engagement without excessively increasing torque requirements. The 70° angle represents a balanced compromise between cutting effectiveness and manufacturing simplicity.

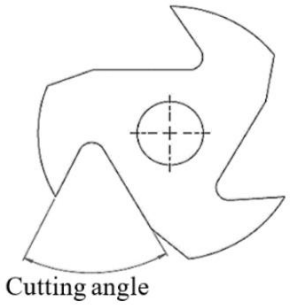

Figure 2 ***Cutting Angle***

Reprinted from Wong et al. (2022)

Grabbing Surface Shape:

A flat grabbing surface was selected. As opposed to the cutting angle, the grabbing surface refers to the shape of the surface of the cutting edge (Wong et al., 2022, p. 5). Compared to curved surfaces, flat surfaces distribute stress more evenly across the blade, reducing long-term wear and tear and prolonging the operational life of each blade. Additionally, flat surfaces are simpler and cheaper to manufacture.

Blade Thickness:

A 5 mm blade thickness was chosen based on material availability and manufacturing capabilities at the university workshop. This thickness is sufficient for the mechanical loads expected during PLA filament shredding, while minimizing weight and simplifying production.

4.3.2 Blade Arrangement and Cutting Action

Blade Orientation:

A zig-zag blade arrangement was selected, where blades alternate in their angle of rotation along the shaft axis by 90 degrees. Given that two cutting edges per blade have been selected, this blade orientation ensures that half of all blades engage the shredding material at a time. Although direct research is lacking on optimal zig-zag vs. series configurations, a zig-zag setup is expected to improve material engagement and reduce the chance of long, unshredded filament sections, with only a modest increase in assembly complexity.

Cutting Mode – Compression vs. Shearing:

A compression/crushing cutting mode was selected over edge-to-edge shearing. This choice reflects the project's focus on robustness, ease of manufacturing, and maintainability. Compression shredding is less sensitive to blade alignment and wear, and is more forgiving in a student-operated environment.

Rotating vs. Static Blade Configuration:

Rotating blades will be arranged between static blades. This configuration simplifies the frame structure, facilitates easier shaft removal for maintenance, and reduces the risk of filament buildup and heat-induced melting along the shredder walls.

Blade Mounting Method:

The shredder will use a spacer ring system between rotary blades. Blades will be spaced evenly along the shaft by precision metal rings, and the stack will be axially compressed by the shredder's side walls. This design allows fast blade replacement without dealing with bolt loosening or weld failures. Careful attention will be given to ensuring torque transfer between the shaft and blades, potentially through the use of keyed shafts or matching flats. This system simplifies assembly, improves maintainability, and supports modular design goals.

Blade Replacement Strategy:

Full shaft removal was selected as the blade replacement strategy, corresponding to the blade mounting method. While individual blade removal would theoretically allow faster servicing, practical constraints related to access, bolt loosening under vibration, and mechanical layout make the full shaft removal the safer and more reliable option.

4.3.3 Material Selection and Surface Treatment

Blade Material:

Tool steel was selected for the blades. This material provides excellent hardness and wear resistance without requiring additional surface treatments, such as hardening or coating, which could be challenging to implement reliably within university resources. Preliminary discussions with supervisor confirmed the feasibility of sourcing hardened steel.

Surface Treatment:

No additional surface treatment or coating will be applied. The inherent properties of tool steel are sufficient for the expected loads and operational environment of PLA shredding.

4.3.4 Flake Size and Cutter Clearance

Target Flake Size:

A fine flake size of ≤5 mm was targeted to ensure compatibility with re-extrusion workflows and to align with closed-loop recycling objectives. Although generating finer flakes may increase shredding difficulty slightly, it is necessary to produce feedstock suitable for high-quality filament production.

Cutter Clearance:

A medium cutter clearance of approximately 0.1-1.0 mm per side was chosen, and a more precise clearance will be selected further along in the design process, as narrowing the clearance size down is dependent on the overall

shredder compartment geometry. This provides a reasonable balance between achieving a consistent flake size and minimizing the risk of jamming. Smaller clearances (<0.1 mm) risk excessive friction and blade wear, while larger gaps (>1.0 mm) may lead to inconsistent flake sizes or tearing instead of clean cutting. Given the use of a capturing sieve for oversized flakes, occasional deviations in flake size are acceptable without impacting the overall recycling process.

4.4 Motor and Transmission Concept

4.4.1 Target Shaft Speed (RPM)

The shaft rotational speed for the filament shredder must balance two critical factors: minimizing frictional heating to prevent PLA softening and ensuring sufficient material throughput for practical laboratory use.

Polylactic acid is a thermoplastic polymer with a relatively low glass transition temperature, typically around 60°C (Song et al., 2017). Excessive frictional heating at the blade interfaces could cause localized softening or partial melting of the material, leading to clogging, poor flake quality, and operational downtime. Therefore, the shaft speed must be low enough to minimize frictional heating while maintaining acceptable shredding efficiency.

Empirical observations from small-scale DIY shredders support this design consideration. The Next Layer (2024) recommends a shaft rotational speed range of 30-70 RPM based on practical testing and operational experience with PLA and other 3D printing materials. This range balances throughput with thermal safety, avoiding material softening during shredding.

Considering these factors, a target shaft speed of 50 RPM was selected for this project. This value sits at the midpoint of the recommended operational range, ensuring low frictional heating while providing sufficient throughput for laboratory-scale recycling operations. Additionally, a 50 RPM target simplifies gearbox selection and motor sizing during the detailed design phase.

4.4.2 Design Assumptions

In order to estimate the torque required at the shredder shaft, several geometric and material assumptions must be defined based on the mechanical design, the expected operational scenario, and the target material properties. These assumptions are grounded in the literature discussed in Chapter 2 and the design decisions established in Chapter 4.

- **Blade Diameter:** The cutting radius is 125 mm, corresponding to the 250 mm blade diameter defined in Section 4.3.1. This radius serves as the lever arm in the torque calculations.
- **Total Number of Blades:** The shaft is assumed to carry a total of 10 blades. This number balances cutting efficiency, shaft length constraints, and the torque required per blade. It also allows a reasonable material feed rate while ensuring that not all blades are simultaneously under load. Based on the zig-zag blade arrangement, it is further assumed that five blades are actively engaging material at any given time.
- **Cutting Engagement Area:** The engagement area per blade is approximated as a rectangular cross-section, defined by the blade thickness (5 mm) and an assumed cut depth of 5 mm. This depth is chosen as a representative middle-ground value to accommodate a variety of PLA scrap geometries, including partial perimeters, infill walls, and structural fragments. While real engagement will vary with feed material shape, this value provides a conservative basis for calculation.
- **Number of Blades in Contact:** The shredder employs a single-shaft layout in a zig-zag pattern. It is assumed that at any given moment, half of the blades are actively engaging with material. This assumption aligns with the geometric arrangement of the blade stack and is supported by common design practice in small-scale shredders.
- **Shear Strength of PLA:** Based on experimental data reported by Torres et al. (2015), the shear strength of 3D-printed PLA with 100% infill ranges between 39.42 MPa and 53.35 MPa depending on raster angle and build parameters. A conservative value of 40 MPa is selected for this design to ensure that the torque estimate reflects the upper

bound of common failure thresholds while remaining within observed material behaviour.

- **Failure Mode:** The design assumes that PLA failure during shredding is governed by shear, which is consistent with the operational mechanics of rotary blade shearing and the known brittle behaviour of PLA under stress.
- **Safety Factor:** A safety factor of 1.50 is applied to the final torque value. This accounts for uncertainties in material variability, engagement conditions, and potential loading peaks during startup or irregular shredding events.

These assumptions define the basis for the torque estimation method made below.

4.4.3 Calculation Procedure and Interim Results

The objective of this subsection is to translate the material and geometric assumptions defined in Section 4.4.2 into a single numeric torque requirement (T_{design}) that subsequent component-selection chapters must satisfy.

Step 1 – Cutting area per blade

The instantaneous shear area engaged by one blade edge is approximated as a rectangle equation (1).

$$A_{\text{blade}} = d \cdot b, \tag{1}$$

Where A_{blade} represents the engaged cutting area per blade, d is the depth of the blade, and b is the blade thickness.

Substituting d = 5 mm and b = 5 mm (from assumptions made in Section 4.4.2) gives

$$A_{\text{blade}} = 5\ \text{mm} \cdot 5\ \text{mm} = 25\ \text{mm}^2$$
$$= 2.5 \cdot 10^{-5}\ \text{m}^2$$

As shown in equation (2), because five blades are assumed to act simultaneously, the total engagement area becomes

$$A_{\text{tot}} = N_{\text{engaged}} \cdot A_{\text{blade}}, \tag{2}$$

Where total engagement area is represented by A_{tot} and the number of simultaneous engaged blades is N_{engaged}.

Therefore, substituting $N_{\text{engaged}} = 5$ and $A_{\text{blade}} = 2.5 \cdot 10^{-5}$ m^2 gives

$$\begin{aligned} A_{\text{tot}} &= 5 \cdot 2.5 \cdot 10^{-5}\ \text{m}^2 \\ &= 1.25 \cdot 10^{-4}\ \text{m}^2 \end{aligned}$$

Step 2 – Shear force

Using the conservative PLA shear strength $\tau_s = 40$ MPa (Torres et al., 2015), the total shear force F_{shear} is, according to equation (3),

$$F_{\text{shear}} = \tau_{\text{shear}} \cdot A_{\text{tot}}, \tag{3}$$

$$\begin{aligned} F_{\text{shear}} &= 40 \cdot 10^{6}\ \text{Pa} \cdot 1.25 \cdot 10^{-4}\ \text{m}^2 \\ &\approx 5000\ \text{N} \end{aligned}$$

Step 3 – Base Torque

The cutting radius equals half of the 125 mm blade diameter. The torque generated at the shaft can therefore be calculated using equation (4).

$$\tau_{\text{base}} = F_{\text{shear}} \cdot r, \tag{4}$$

Where τ_{base} is the torque generated at the shaft and r is the cutting radius.

Substituting $F_{\text{shear}} = 5000$ N and $r = 0.125$ m gives

$$\begin{aligned} \tau_{\text{base}} &= 5000\ \text{N} \cdot 0.125\ \text{m} \\ &\approx 625\ \text{N·m} \end{aligned}$$

Step 4 – Design torque with safety factor

Applying the project safety factor of 1.50 as per equation (5) gives the final requirement:

$$\tau_{\text{design}} = \tau_{\text{base}} \cdot 1.50, \tag{5}$$

Substituting $\tau_{\text{base}} = 625$ N·m gives

$$\tau_{\text{design}} = 625\ \text{N·m} \cdot 1.50$$

$$\approx 9.375 \cdot 10^2 \text{ N·m}$$

Interim result – The shredder shaft shall be capable of transmitting τ_{design} **= 937.5 N·m** at the nominal operating speed of 50 r·min^{-1}.

4.5 Material Collection System

A removable bin module was selected for the shredder's output collection. The compartment will be dimensioned to accept a standard laboratory storage bin at its output for the collection of flakes, allowing flakes to be stored in bulk while awaiting recycling and re-extrusion. The bin slides out on linear guides that constrain it in all three axes: between the floor plate, side walls, back walls, and enclosure door. This design allows an operator to exchange a full bin in under 10 seconds, minimising downtime and enabling near-continuous operation of the shredder.

Above the bin, a sieve is mounted at a shallow incline. It is perforated with 5 mm holes to ensure that only flakes meeting the re-extrusion requirement defined in Section 4.3.4 (≤5 mm in any axis) fall into the primary bin, while oversized particles slide into a secondary catch tray for manual reprocessing.

4.6 Safety and Sensor Systems

Ensuring operational safety and reliable detection of faults is critical in the design of shredding equipment, particularly within educational environments where operators may have varied technical proficiency. This section outlines the safety and sensing features integrated into the shredder design, with an emphasis on preventing injury, detecting abnormal operating conditions, and protecting the mechanical components from damage.

4.6.1 Interlocking Lid System

To minimize operator risk during operation, a lid interlock system was incorporated. This mechanism uses a position sensor (i.e. reed switch or limit switch)

to detect whether the shredder lid is securely closed. When the lid is open, the interlock circuit remains open, effectively preventing motor activation regardless of the control button status. This incorporation ensures that access to the rotating blades is blocked during operation.

4.6.2 Emergency Stop Circuit

An emergency stop (E-Stop) button is included as a primary fail-safe. The button is wired through a safety relay to cut off power to the motor immediately when pressed. This setup ensures that the system cannot resume operation without manual reset, and it conforms to standard industrial safety practices for electromechanical systems.

4.6.3 Rotary Encoder for Shaft Rotation Detection

To monitor whether the shredder shaft is rotating during operation, an incremental rotary encoder is mounted on the motor output shaft. The encoder provides pulse feedback to a microcontroller, which tracks whether rotation is occurring. If the system detects an absence of encoder pulses for a defined time interval while the motor is energized, a fault condition is triggered.

4.6.4 Current Sensing for Overload Detection

In addition to mechanical motion sensor, electrical current monitoring is implemented to detect motor overload or potential shaft jamming. A Hall-effect current sensor is installed in-line with the motor’s power supply. During normal operation, current readings are logged and analysed to establish a baseline. If the system detects a spike in current beyond expectation, it is interpreted as a jam or excessive load, prompting an automatic shutdown. This method provides an additional layer of protection and is particularly useful when mechanical sensing alone is inconclusive.

4.6.5 Control Integration and Logic

All safety and sensor components are interfaced with a microcontroller (i.e. ESP32 or Arduino Uno), which processes sensor inputs and control motor activation via relays or motor drivers. The firmware includes safety checks that validate lid position, encoder pulse activity, and current levels before and during operation. In any fault condition (such as an open lid, shaft stall, or overload), the system enters a fault state, disables the motor, and requires a manual reset. This approach ensures redundancy in safety systems.

4.7 Final Concept Description

The final shredder concept consolidates all the design decisions made throughout the conceptual and component selection phases into a single unit tailored for laboratory-scale filament recycling. The machine consists of a single-shaft shredding mechanism, a motor and gearbox assembly selected based on detailed torque calculations, and integrated safety and sensing systems suitable for use in educational environments.

The shredding mechanism features a 250 mm blade diameter with a total of 10 blades arranged in a zig-zag pattern. Each blade has two flat cutting edges positioned at a 70° angle at the shaft axis, producing cutting action suitable for PLA. A tight clearance is maintained between adjacent blades and the casing to improve cutting efficiency while reducing the likelihood of jamming. The blade thickness and cut depth are each set to 5 mm. These parameters, combined with an assumed engagement of five blades per cut, form the basis of the torque calculations described in Section 4.4.3.

The shaft transmits a peak design torque of 937.5 N·m at 50 $r \cdot min^{-1}$, as derived from material strength data, blade geometry, and the applied safety factor. This requirement directly informs the motor sizing and gearbox ration exploration. Depending on what motors or gearboxes are available at the laboratory, gear ratio calculations can be performed to ensure the selected motor delivers the required torque at the target operating speed.

Material output is collected in a removable bin beneath the cutting chamber. The bin slides on constrained linear guides and is topped with a perforated

inclined sieve that filters oversized flakes, ensuring only flakes ≤ 5 mm are collected for re-extrusion.

Safety features include an interlocking lid detection system, an emergency stop button wired through a safety relay, a rotary encoder to detect shaft rotation, and a Hall-effect current sensor for overload detection. All sensor outputs are process via a microcontroller that governs motor control logic and fault response.

This finalized configuration meets the laboratory's sustainability goals, supports batch processing of PLA waste, and provides a flexible platform for future expansion or sensor integration. The design also emphasizes accessibility, maintenance ease, and adaptability to existing lab infrastructure, ensuring the concept is both technically sound and practically feasible.

5 COMPONENT SELECTION AND MATERIAL CHOICES

5.1 Introduction

This chapter covers the selection of every major component used in the design of the shredder, from mechanical parts such as the shaft and bearings to electronics like the microcontroller and sensors. While the original plan involved some rough assumptions about blade sizing, frame layout, and material types, many of those changed throughout the design process and constraints became clearer and priorities shifted. Cost, local availability, time limitations, and ease of manufacturing played a major role in determining what was actually feasible.

The goal of this section is to explain why each component was chosen, how it fits into the overall system, and what trade-offs were made. This includes the switch from tool steel to regular structural steel, the final choice of a 25 mm shaft, and the use of modular off-the-shelf parts wherever possible to simplify and reduce the manufacturing and assembly complexity. The entire system

was designed around practical constraints, with a focus on getting it done without sacrificing any key functionalities or safety.

5.2 Mechanical Components

5.2.1 Blade Geometry and Material

The blade diameter was originally set to 250mm, mostly based on theoretical torque and cutting depth calculations early on in the project. Once the rest of the design started coming together, it became clear that 250 mm was oversized for a desktop-scale machine. The diameter was thus reduced to 125 mm, which significantly reduced the required torque and allowed the shredder to be more compact without sacrificing cutting performance for small-format prints and support structures.

As for material, the original plan was to use tool steel. Once cost, lead time, and available tooling at the university were taken into account, this idea was scrapped in favour of using normal mild steel. This type of steel is easier to machine and available locally at the required thicknesses at a more cost-friendly figure. While it does not have the same wear resistance or hardness as tool steel, it is more than sufficient for prototyping and test use, especially given that PLA is the only material that will be shredded.

5.2.2 Shaft

The shaft diameter remained at 25 mm, matching standard bearing and coupling sizes. This size was chosen because it provides a good balance between torsional strength and part availability.

5.2.3 Bearings

The shaft is supported by UCP205 pillow block bearings on both ends. These bearings are widely available, easy to install, cost-effective, and offer more than enough load capacity for this application. They are mounted on horizontal

support struts and secured with M10 bolts. Bearing positioning was aligned with the final shaft length and shredder compartment width, and the setup leaves just enough clearance to mount the encoder at the rear end of the shaft.

5.3 Drive System

5.3.1 Motor and Gearbox

The motor and gearbox used in the 3D model are placeholders representing a compact industrial gearmotor suitable for the required torque and speed range. The model used is based on the SEW-Eurodrive R77 with a DRE90L4 motor, selected due to its compatibility with standard couplers and bearings, and it its known performance characteristics. However, the actual motor and gearbox to be used will depend on what is available at the university lab.

The motor is mounted using a dual-plate standoff structure supported by four M16 threaded rods. This design is simple, rigid, and allows for easy adjustments of motor position while maintaining proper alignment with the saft. The motor is placed on the right side of the shredder body, outside the main frame which significantly increases the footprint but simplifies maintenance and assembly.

5.3.2 Torque Transmission

Torque is transmitted form the motor to the shredder shaft through a flexible jaw-type coupler. The specific coupler modelled is an L150 type with 25 mm keyed bores on both ends. Like the motor and gearbox, this coupler is also considered a placeholder, and the final selection will depend on what is available in the lab inventory.

This type of coupler was selected because it allows for minor misalignment and axial play, which is necessary in a welded frame structure where perfect alignment is difficult to guarantee. Its use improves durability and reduces stress on the motor bearings and shaft supports.

Following the reduction of the blade diameter from 250 mm to 125 mm, the required torque was recalculated. Since torque scales linearly with blade radius under the same cutting conditions, and the blade radius is the only torque-affecting component that was modified, the torque requirement was reduced by half. This confirmed that the selected placeholder motor and coupler configuration still provides more than enough headroom.

5.4 Structural Frame and Panels

5.4.1 Frame Tubing

The frame is constructed using 30 x 30 mm mild steel square tubing. This profile was chosen because it is readily available, easy to weld or drill into, and strong enough to support the full assembly, including the shredder shaft, motor, gearbox, and outer panels. Larger profiles were not considered necessary given the reduced blade diameter and overall system weight.

The frame was designed to accommodate internal mounting of all subsystems, including the bearing supports, sieve struts, and panel brackets. Rather than building the structure as a uniform cube, the frame geometry was adapted to fit the actual size of the shredding chamber and to reduce wasted space and material. This resulted in a custom, asymmetric footprint that remains compact but better suits the mechanical and functional layout of the machine.

Multiple horizontal and vertical cross-members were included for reinforcement and to provide mounting points for components such as the bin access door, motor platform, and sieve.

5.4.2 Panel Material and Mounting

Panels are assumed to be made from mild steel or thin aluminium sheets, depending on availability. These panels are mounted to the frame using 3D printed corner brackets. Each bracket is secured to the frame using M5 bolts, and threaded heat-set inserts were embedded into the brackets to allow for panel removal and reinstallation without compromising on durability.

For corner junctions, offset rivet spacing and lapped panels were used toa void interference and allow clean edge alignment. In locations where the panels were specially shaped, such as the triangular panels of the oversized bin chute or the hopper, specially designed brackets were added to suit the geometry instead.

The front of the machine includes a hinged bin access door, and the electronics enclosure includes a hinged handle lid with a handle and locking bolt. The top feeding lid is also hinged, with an integrated magnet and reed switch bracket to support the lid interlock safety system.

The modular and serviceable panelling approach was selected to allow access to internal components while maintaining a clean and fully enclosed external structure.

5.5 Sensor and Electronic Component Selection

5.5.1 Microcontroller

The system is controlled by an Arduino Uno, selected for its simplicity, compatibility with all required sensors, and ease of programming. While more advanced microcontrollers such as the ESP32 were considered during early stages of planning, the Arduino Uno was ultimately chosen due to its reliability, straightforward setup, and author familiarity. It provides more than enough digital and analogue I/O for the sensors used and is well supported in both hardware and software resources.

5.5.2 Safety and Feedback Systems

The shredder incorporates multiple safety systems and monitoring sensors, all of which were included in the 3D model. A 22 mm emergency stop button is mounted on the side panel and connects through a relay circuit to ensure immediate shutdown in case of fault or emergency. A start button, also 22 mm, is placed below the E-stop and provides user control over system activation.

Both buttons are industrial off-the-shelf components mounted through panel cutouts.

A reed switch and neodymium magnet pair from the lid form the lid interlock system. When the feeding lid is opened, the magnet moves away from the sensor, breaking the circuit and disabling the system through the relay control logic. The reed switch is mounted inside a custom 3D printed housing bolted to the hopper wall, and the magnet is mounted in a matching bracket on the underside of the lid.

A rotary encoder is mounted to the free end of the shaft and is used to monitor rotation and detect potential jamming. The encoder body is mounted to a bracket that is fixed to the shredder frame.

To monitor current draw and detect overload conditions, an ACS712 current sensor module is placed inside the electronics box. It measures current flowing to the motor through its terminal block and provides analogue feedback to the Arduino. This allows the system to detect sustained overcurrent conditions and trigger a shutdown sequence if necessary.

5.5.3 Power and Control

Motor control is handled directly through the Variable Frequency Drive (VFD), which includes a built-in relay interface for external safety devices. The emergency stop (E-stop) button is hardwired to the VFD's safety input, allowing immediate shutdown of motor output in case of an emergency. This hardware-level integration ensures that the motor is safely and reliably disabled without relying on software logic alone.

The Arduino microcontroller is responsible for managing safety monitoring and interfacing with other components, such as the interlock switch and overload detection system (based on current sensing). Rather than controlling power directly, the Arduino sends logic-level signals to the VFD's digital input terminals to enable or disable motor operation based on system state.

All control electronics are housed within a dedicated electronics enclosure, ensuring both safety and serviceability.

5.6 Summary

This chapter detailed the selection of all major components and materials used in the design of the shredder. Mechanical components were chosen with a focus on compatibility, local availability, and ease of fabrication. The final system uses a 125 mm blade diameter and a 25 mm shaft, supported by standard UCP205 bearings and connected via a placeholder jaw-type coupler representing what is expected to be available in the lab.

The drive system was modelled around a placeholder SEW-Eurodrive motor and gearbox assembly, mounted externally on a dual-plate frame. Torque requirements were reassessed after the blade size reduction, confirming that the modelled components provide sufficient margin. All torque transmission elements, including the shaft and coupler, were selected accordingly.

The structural frame uses 30 x 30 mm mild steel tubing, with bolted panelling supported by custom 3D printed brackets. Hinged panels and access doors were added to simplify maintenance and allow internal access.

Electronic components were selected to meet safety, control, and feedback requirements. An Arduino Uno handles logic control, with supporting sensors for lid position, shaft rotation, and motor currents. All sensors and interfaces were modelled, and the electronics are enclosed in a serviceable box mounted to the frame.

Overall, the selected components reflect the system’s functional requirements while accounting for budget, manufacturing feasibility, and time constraints.

6 DETAILED DESIGN AND MODELLING

6.1 Introduction

The detailed design and modelling phase formed the core of the thesis, occupying the majority of the project’s execution timeline. Every mechanical, electronic, and structural element of the shredder was modelled using SolidWorks 2024, with the primary goal of producing a functional, ready to build digital

prototype that could be used as a direct and standalone basis for physical manufacturing. While the initial plan was to proceed directly to construction, limited availability of components and fabrication time required that the model be the final deliverable.

This chapter documents the full modelling workflows, including the structure or of the assembly, the reasoning behind part configurations, modelling strategies for key subsystems, and the iterative design decisions made to resolve issues of tolerance, alignment, and manufacturability. Each part and subassembly was created with real-world tolerances in mind, with particular attention given to parts subject to mechanical stress or motion.

The modelling process involved frequent trial and error, especially when adapting components to standard dimensions and ensuring proper clearance between moving parts. Special care was taken to standardize similar components using configurations: the outer panels, inner panels, spacers, and static blades. This allowed geometry to be reused while accommodating design-specific variations.

6.2 Assembly Structure and Workflow

The shredder model was constructed as a multi-level hierarchical assembly in SolidWorks. Each major subsystem, such as the frame, shaft, blade stack, and motor system were created as a distinct subassembly, stored in separate part and assembly files for clarity and ease of iteration. Second-level assemblies, such as panel brackets, were modelled within their immediate parent subassembly. This modular structure allowed clean modifications while preserving parametric control over dimensions and relationships.

From the very beginning, the modelling process emphasized parametric design. Almost every dimension was controlled using equations and global variables, and design tables were used to manage configurations where multiple variants of a part were required. Examples of parts modelled with configurations include the panel brackets, static blades, inner wall panels, outer wall panels, and blade spacers. This approach reduced part duplication, ensured

dimensional consistency, and accelerated design updates, especially after several system-wide geometry changes.

All files were named according to standardized convention, as seen in Figure 3. Assembly files were suffixed with “Assembly”, with the exception of the top-level assembly file, simply titled “Shredder”. Part naming was internally consistent, although a blend of lowercase underscored and capital with spaces was used depending on when the part was created. Throughout the workflow, great care was taken to maintain clarity in the feature tree and mate structure, even during periods of rapid iteration.

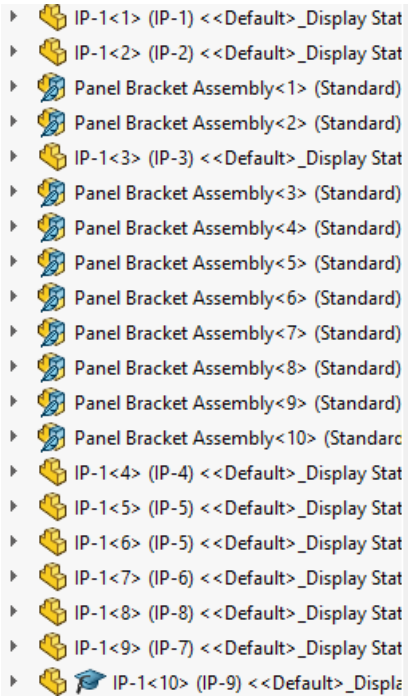

Figure 3 Top-level assembly feature tree hierarchy

Model complexity increased significantly as more components were added, particularly toward the final stages of development. As a result, SolidWorks became increasingly unstable, with crashes occurring multiple times per day during the final two days. Nonetheless, diligent versioning and near-constant manual saves prevented significant data loss allowing progress to continue, despite some time-related setbacks. Frequent lag during part placement and mating slowed progress but did not block the completion of the model.

Initial modelling began without finalized system dimensions or fixed hardware parameters. As a result, a significant portion of the design process was exploratory and evolved in real time. For instance, the overall footprint of the shredder had to be reduced midway through the process to ensure alignment

reliability and build feasibility. These decisions were not made from a top-down system specification but rather through iterative modelling, testing, and adjustment.

6.3 Structural Frame and Panel Integration

The structural frame was designed as a single part using extrusions, as seen in Figure 4. Each strut was created as a solid body with hollow interiors to reflect the use of square steel tubing in the physical build. Although the weldments features of SolidWorks were not used, the frame served the same functional role, with careful attention paid to manufacturability and realistic geometry.

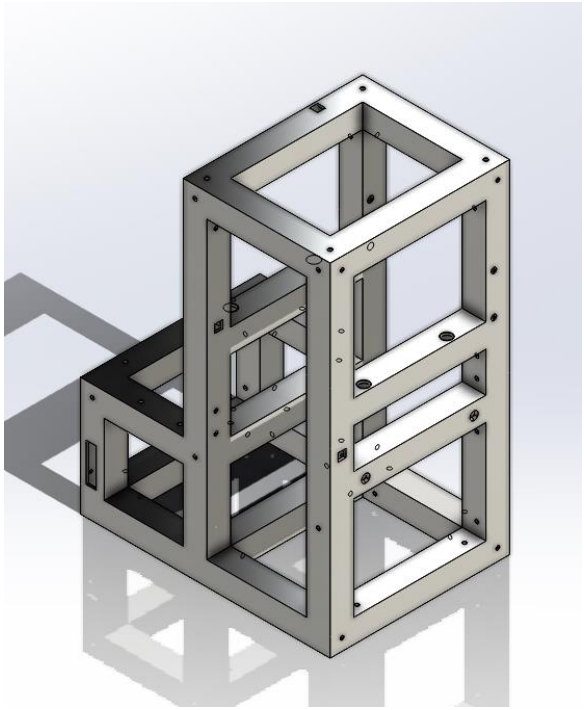

Figure 4 Frame model including holes for bolting and cutouts for wire channels and spacing

A custom naming convention cand labelling system was used to organize frame elements and guide physical cutting. Each strut was labelled according to its level (0 for bottom, 1 for first level above the bottom, up to level 3 for top level), orientation (front, back, left, right, or a combination), and type (horizontal or vertical), such as “1FRV” for “Level 1, Front Right Vertical”. This labelling system was created to enable the efficient identification of and working with

struts during real-world manufacturing, especially under tight deadlines and with multiple people involved.

Most panels were designed from two standardized parts, the inner panel template and the outer panel template which can be seen in Figure 5, each of which had a standard dimension set and bolt holes. All panels were created from these templates by adjusting the configuration-specific dimensions, bolt hole amount, locations, and sizing, alongside any other required extrusions due to special panel shapes such as angled panels and non-rectangular panels. The button mount panel was designed separately using the SolidWorks sheet metal features to ensure proper flattening for plasma cutting due to its unique box shape. Brackets were added to provide attachment points for panels, electronics, and rotating components. Brackets of a specific purpose (i.e. panel brackets) were generally standardized using configurations where possible for standardized dimensions and bolt hole locations and were designed for 3D printing due to the relatively light loads of aluminium panels or light electronics, especially as four brackets would be used per panel.

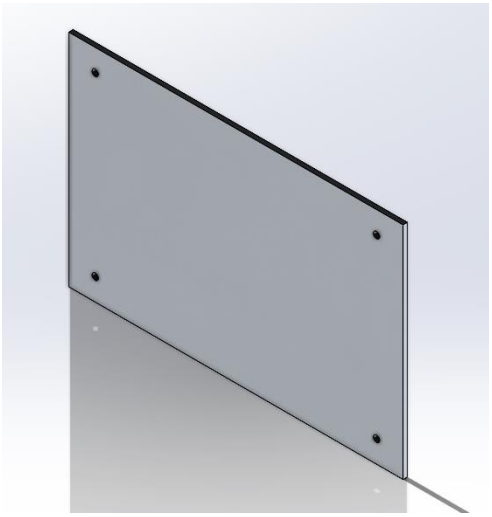

Figure 5 The template for the outer panels

Clearances were handled through parametric tolerancing. An offset of 0.05mm was applied to metal parts to ensure manufacturability, and all panel slots and holes used the SolidWorks hole wizard feature to ensure compatibility with standardized ISO bolts and nuts. These design decisions allowed for rapid assembly with standard workshop tools and accounting for the inherent variability due to welding steel frames and 3D printing.

6.4 Shaft, Blades, and Shredding Compartment

The shredding mechanism (Figures 6 and 7) consists of a rotating shaft mounted with a stack of rotary blades and spacers of multiple types. This sub-assembly required the highest level of precision in the model due to its mechanical complexity and tight tolerance requirements.

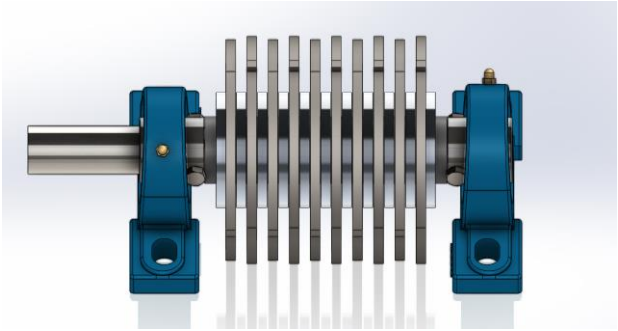

Figure 6 Top-forward view of the shaft assembly

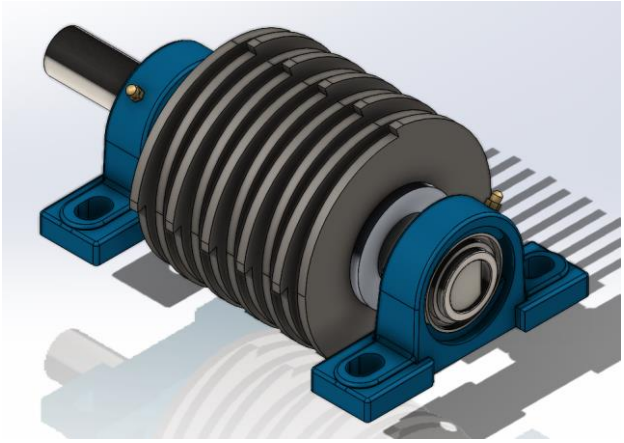

Figure 7 Isometric view of the shaft assembly

The shaft itself was modelled as a single steel rod with a diameter of 25 mm, supported at both ends by UCP205 bearings. To provide a leveraging surface for the rotary blades and spacers for the shaft to transmit rotational forces, a flat cutout was added along the entirety of the shaft, with a matching flat section in the shaft slot of each component running along it. Due to time constraints and modelling complexity, the UCP205 bearings were sourced from a CAD-sharing website as it is standardized in size and function.

6.4.1 Blade and Spacer Stack

The rotating blade stack was designed using 5 mm thick steel discs with plasma-cut cutting edges. Originally, 6 mm steel spacers were used between each blade, but this was later modified to a hybrid approach of 5 mm steel spacers plus 0.5 mm 3D printed PETG spacers on each side of the steel spacer to account for a lack of 6 mm steel plates. This redesign simplified material sourcing while allowing for fine-tuning of axial spacing if needed.

To eliminate unwanted friction and account for minor alignment tolerances, the static blades (Figure 8) which were initially 5.8 mm and 5.2 mm thick depending on position were redesigned to be 5.0 mm thick. This change introduced a consistent 0.5 mm clearance between rotary and static blades on either side, significantly improving reliability and ease of processing.

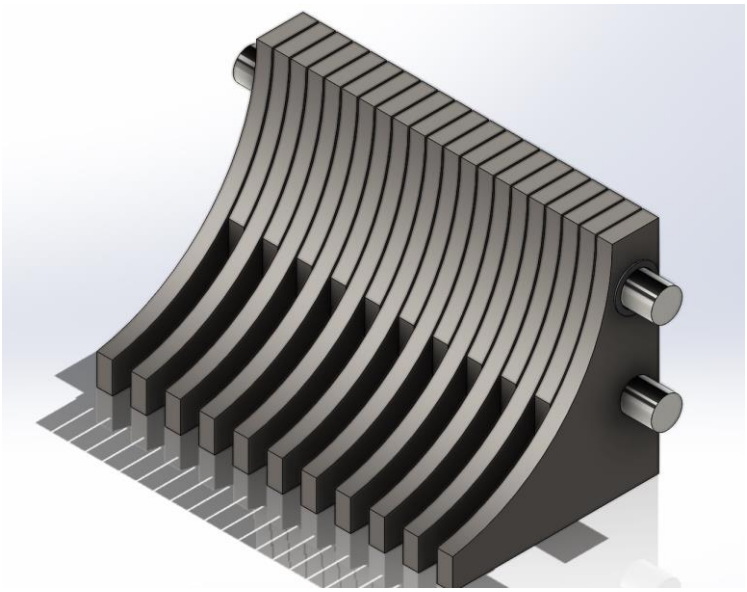

Figure 8 Static blade stack

6.4.2 Shaft Redesign

The original constraint method relied on wall panels pressing against the outermost spacers to lock the shaft blades in place. This approach created excessive friction and introduced dependencies on precise welding and panel tolerancing. It was ultimately replaced with a more robust constraint system.

Printed compression spacers were introduced between the inner bearings and the outermost steel spacers. These compression spacers eliminated the need

for wall-constrained locking, shifting the constraint to the bearing itself. To accommodate the new spacer, the hole in the wall panels were enlarged, and the outermost metal spacers' thicknesses were reduced to roughly 5.8 mm to prevent any risk of contact with the panel.

6.4.3 Static Blade Integration

Static blades are pressed and aligned between two opposite wall panels in the shredding compartment and held up by two steel brackets as shown in Figure 9, each bolted to the frame on either side that hold the two rods of the static blade stack in place, preventing lateral and rotational motion. Each blade is surrounded by a 0.5 mm spacer to ensure a consistent 0.5mm clearance between each static blade and its rotating counterpart.

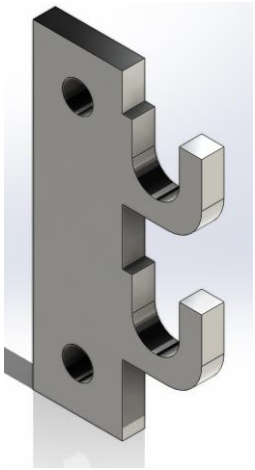

Figure 9 Static blade bracket

6.5 Motor and Mount

The power transmission of the shredder consists of a geared AC motor connected to the shaft through a flexible jaw-type coupler. Although the final components to be used at the university were not confirmed at the time of modelling, nor was there an online 3D model of the available motor once confirmed, placeholder models were incorporated to reserve accurate space and ensure a functional layout. The decision to not model the motor itself was made due to time constraints.

The placeholder motor-gearbox unit used in the model is an SEW-Eurodrive R77 DRE90L4, selected for its integrated gearbox and sufficient torque output. The motor itself is mounted horizontally on the right-hand side of the shredder. The motor mount consists of two thick steel plates separated by a set of threaded rods to provide variability in the motor height. The motor mount assembly, including the mount, motor, gearbox, and coupler is shown in Figure 10.

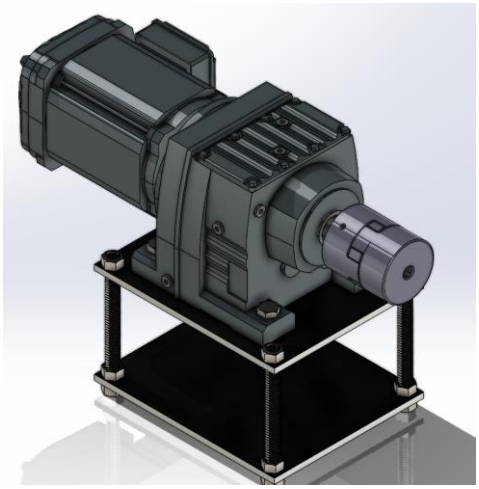

Figure 10 Motor assembly

The shaft is connected to the gearbox using a placeholder model of a Lovejoy L150 jaw-type coupler. The coupler was selected for tis flexibility and self-aligning feature, which mitigate the risk of angular or axial misalignment during operation which could otherwise damage the motor or shredder shafts. Although the CAD model used did not reflect real bore geometry, it was dimensionally accurate and sufficient for modelling purposes.

6.6 Flake Collection System

The shredder’s flake collection system was designed to separate standard-sized flakes from oversized ones by incorporating a custom-fitted sieve. The system is located directly beneath the shredding compartment and is composed of angled panels that funnel output material into two separate bins: one for standard flakes that pass through the sieve and another for oversized flakes that do not.

The sieve is a flat, perforated sheet (Figure 11) designed using SolidWorks' Fill Pattern feature. The perforations are uniformly distributed to ensure consistency in flake size control. No mesh or dip features were added to the sieve surface, as these could trap flakes and obstruct flow. Instead, a smooth surface was preferred, prioritizing manufacturability and consistent output behaviour.

The hole diameter was selected based on expected flake dimensions and aligned with standard filament extrusion requirements. Oversized flakes are expected to be rare and will fall into a secondary bin, enabling reprocessing if needed. This trade-off ensures operational reliability without risking clogging from irregular flakes.

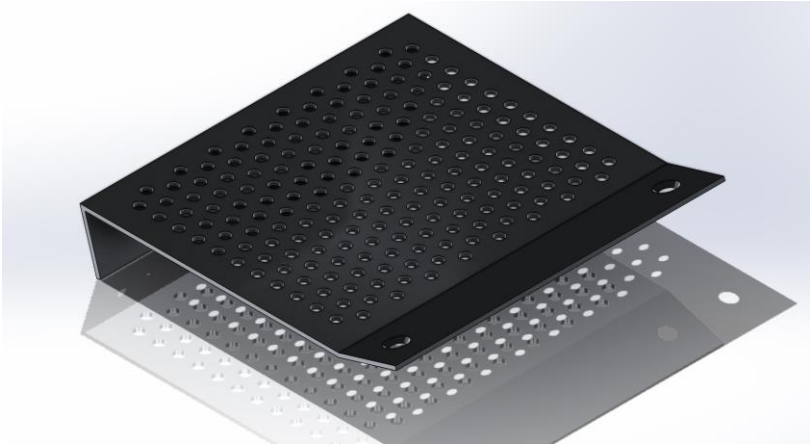

Figure 11 Sieve model

Beneath the sieve, two flake collection boxes were modelled, one directly below the sieve and the other located at the shallow end of the sieve. These containers were designed to ensure that they fit within the surrounding panels and struts without significant regard paid to their storage capacity, as they can easily be removed and emptied through a collection area access panel that is hinged. The system is shown below in Figure 12.

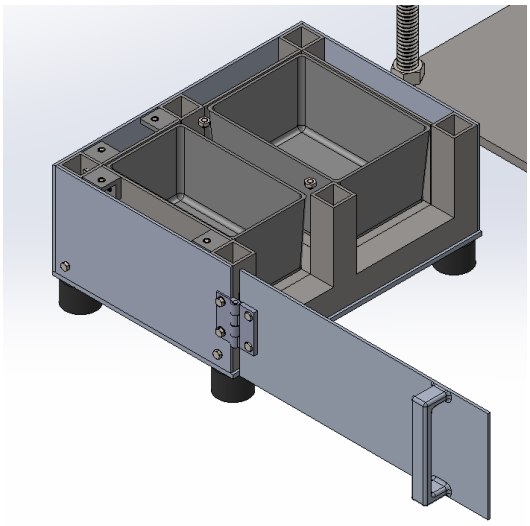

Figure 12 Section view of the collection compartment

6.7 Electronics and Sensor Integration

All electronic component models used were sourced from CAD-sharing websites due to time constraints and due to their standardized nature. Each component relevant to the top-level assembly itself aside from the microcontroller, that is the reed sensor and magnet, rotary encoder, bracket, and housing, were incorporated into the model, while all other electronics, such as the VFD and power unit, were left unmodelled as they would not be located on the shredder itself after real-world assembly.

While wire routing was not physically modelled due to software limitations, dedicated wire channels and accessible component placement were prioritized. The electronics system includes control, power, sensing, and safety hardware, all placed with realistic mounting strategies.

6.7.1 Microcontroller and Housing

The central microcontroller is an ESP32-S3, chosen due to its simplicity and availability in the university laboratory. It is mounted within a custom-designed electronics box located on the side panel of the shredder. The box includes four mounting clips to hold the ESP32 in place, and a cutout in the side of the box for wiring connections. The box was also made to be much larger than the ESP32 to accommodate a safety relay. However, when the available VFD was

later provided, it was found that that it incorporated a safety relay itself. The box was not remodelled due to time limitations, however. Furthermore, due to similar time constraints, the ESP32 model was not incorporated into the model, as the real dimensions were measured with a physical ESP32-S3, and the electronics box dimensions were modelled accordingly.

6.7.2 Buttons

A placeholder set of start, stop, and emergency stop buttons were used as shown in Figure 13, where all of their models were sourced from a model sharing website. These buttons were integrated to represent the real buttons that would be used, a set of Schneider Harmony XB4 buttons for all three. The mounting box for these buttons was modelled using the sheet metal features in SolidWorks to facilitate simple manufacturing with the plasma cutter. The mounting box provides the depth required for the buttons while ensuring they do not interfere with the inner panels. All buttons were positioned to allow for sufficient physical spacing between each for wiring and for the physical geometry of each button.

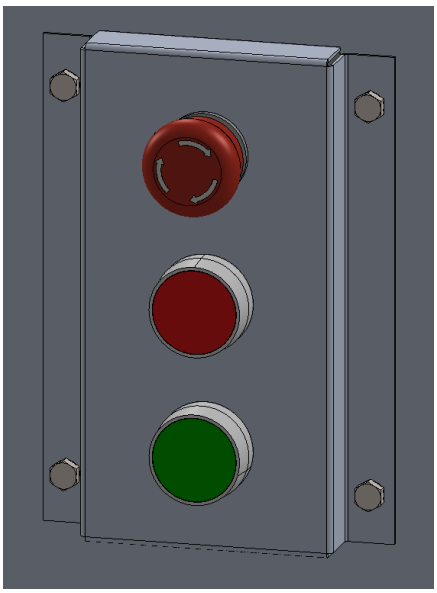

Figure 13 Button panel

6.7.3 Rotary Encoder and Shaft Monitoring

A rotary encoder is mounted at the end of the shredder shaft, opposite of the motor. The encoder was selected to monitor shaft rotation and detect potential jamming. It is mounted via a 3D-printed holder to the frame and aligned to avoid bearing and blade interference. Its placement was determined using the shaft centreline and bearing edge clearances. The mount and encoder are shown below in Figure 14.

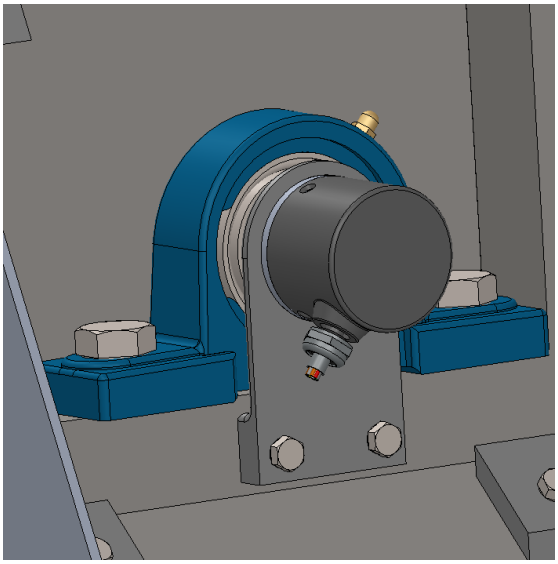

Figure 14 Rotary encoder and mount

6.7.4 Lid Interlock Sensor

A reed switch-based interlock (Figures 15 and 16) was selected to detect whether the lid is securely closed. The sensor is mounted within a dedicated 3D-printed bracket on the frame, while the corresponding magnet is mounted on the lid. Their alignment was tested within the assembly to ensure activation when the lid is closed.

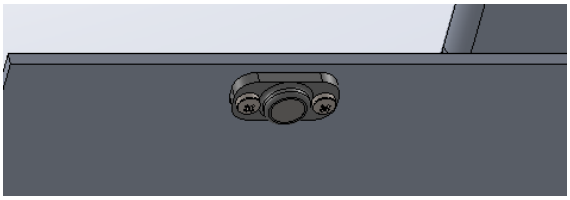

Figure 15 Magnet and Magnet Mount

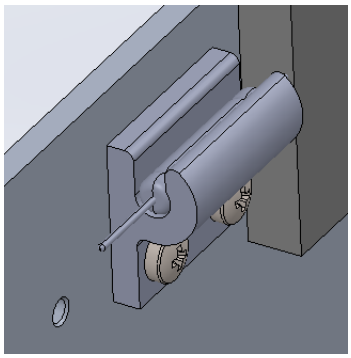

Figure 16 Reed sensor and reed sensor mount

6.8 Design Deviation from Original Plan

While the initial design was based on a general concept of a desktop-sized filament shredder, the final model diverged significantly in geometry, assembly constraints, and component mounting to better reflect real-world manufacturability and available materials. These changes were made during an intensive week-long redesign process after discovering major mechanical limitations in the original concept.

6.8.1 Design Reassessment

The original shredder concept was envisioned as roughly cubic and compact. However, the final model measures approximately 322 mm in length excluding the motor, and roughly 990 mm including the placeholder motor, exceeding the original requirement of a sub-900 mm footprint. This change was however necessary to accommodate the SEW-Eurodrive motor and gearbox while still maintaining correct shaft alignment. The redesigned unit remains desktop-size in terms of footprint and usability.

6.8.2 Blade Geometry and Tolerance Redesign

The rotating blades were originally planned at 250 mm diameter, but were later reduced to 125 mm. This drastically reduced the torque requirement and allowed for easier sourcing of the motor and less usage of material. Furthermore, the static blades were redesigned to be 5.0 mm instead of requiring precision

grinding variants at 5.2 mm and 5.8 mm. Tolerances were introduced between blades to prevent contact with the rotating blades, especially after discovering that the original design relied on panel pressure to constrain axial movement.

6.8.3 Shaft Stack Redesign

The initial concept relied on the shaft stack being constrained between two walls. This method proved unviable due to friction and misalignment risk. It was replaced with a more robust solution using printed compression spacers and regular spacers to maintain the axial positions of the blades and steel spacers, and to maintain alignment with the static blades.

6.8.4 Panel and Button Mounting Adjustments

Several parts of the system had to be redesigned for mounting feasibility. For instance, the buttons required more depth than the 30 mm structural frame could provide. Thus, a button box was designed to protrude from the side panel. Similarly, the electronics box was restructured with better mounting clip reinforcements after the first iteration failed due to print-related stress cracking.

6.9 Summary

The detailed design and modelling phase was the most intensive and iterative component of the thesis. Starting from a conceptual design with numerous assumptions, the project evolved into a robust, manufacturable CAD assembly grounded in mechanical feasibility, part availability, and practical constraints. Over the course of almost two weeks, working from 10 to 14 hours per day, the entire shredder was modelled with a focus on parametric design, tolerance control, and ease of assembly.

Critical mechanical challenges were addressed through multiple redesigns; particularly in the shaft and blade stack, where friction and alignment issues necessitated a significant design change. Standardized subcomponents such as panel brackets and spacers were configured through SolidWorks

configurations to simplify modelling. Every dimension was either derived from linked equations or calculated to ensure accurate fit and function. A full image of the shredder is shown in Figure 17 and a similar image with no panels visible is shown in Figure 18 to showcase the internals of the shredder.

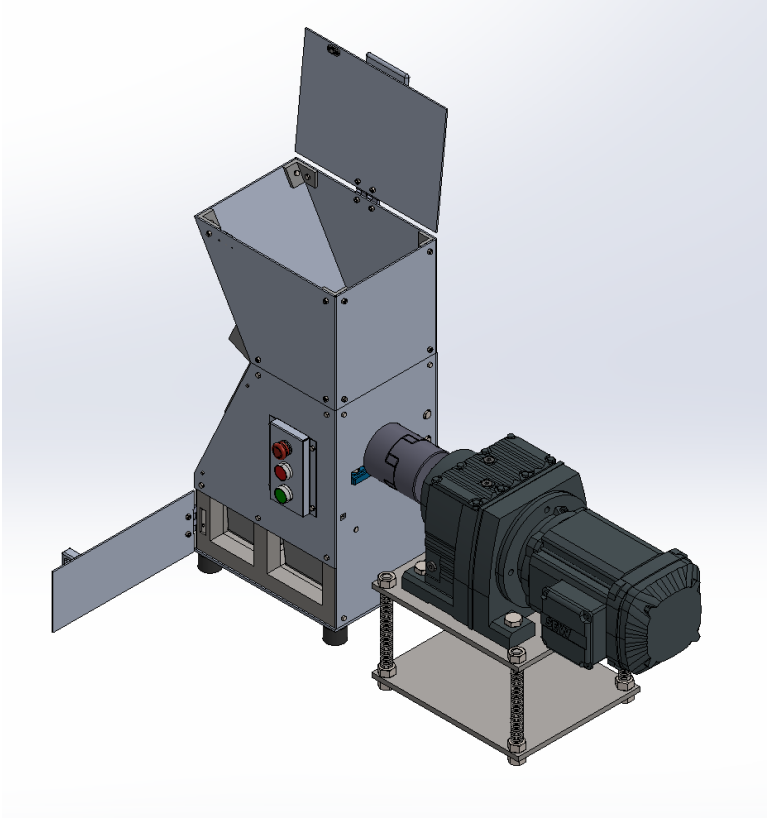

Figure 17 Isometric view of the full shredder

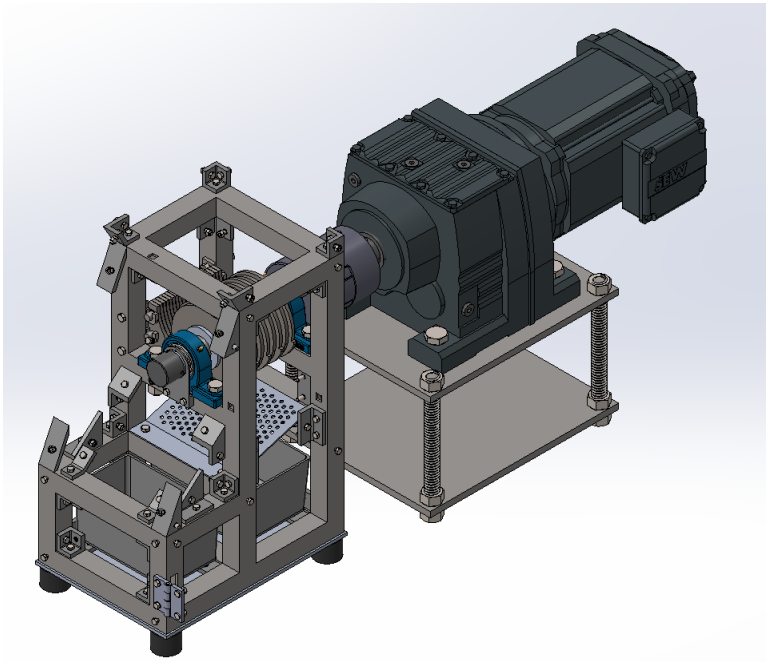

Figure 18 Isometric view of the shredder with panels hidden

Throughout the design, effort was made to prioritize manufacturability including the use of the sheet metal features and the use of mates that replicated real-life mounting physics to ensure that all parts are dimensionally locked using real-world principles over fixed mates.
The result is a complete CAD assembly that not only satisfies the vast majority of the original requirements, but does so with attention to alignment tolerance, material properties, and real-world assembly needs. The design is prepared for manufacturing and physical implementation.

7 BUILD PROCESS AND IN-LAB MANUFACTURING

7.1 Purpose and Scope of the Build Phase

The purpose of this chapter is to document the physical manufacturing of the shredder prototype that followed the detailed modelling work presented in Chapter 6. Whereas the earlier chapter discussed the virtual design work and tolerancing, this chapter records the manufacturing and assembly efforts undertaken during a two week window, from the 14th of May 2025 to the 29th of May 2025. Within this period, the project team balanced hands-on manufacturing with several quick redesigns triggered by unforeseen material and tooling constraints.
Only factual build activities are reported in this chapter. Specifically, this chapter:

- tracks the procurement of materials and the immediate setbacks caused by incorrect materials,
- lists all manufacturing work completed to date; plasma cutting, deburring, surface preparation, and the welding of the first base layer
- distinguishes the work that remains incomplete,
- details the in-process redesigns and adjustments made to accommodate incorrect plate thicknesses and component breakage,

- and records the tool failures encountered, and the workarounds adopted.

7.2 Material Procurement & First-Week Setbacks

The first manufacturing step was to source structural materials; square tubing profiles for the frame and plates for blades, spacers, and panels. The procurement trip on the first build day secured both of these materials, but both introduced immediate obstacles.

7.2.1 Stainless-Steel Tubing Setback

Due to a lack of options, the decision was made to purchase stainless steel tubing rather than mild steel tubing. However, stainless steel's hardness exceeded the abilities of the workshop's cutting equipment. The industrial bandsaw (Huvema BMSY 325C) dulled and slipped by the third cut, while a smaller tabletop bandsaw failed similarly after another few cuts. As a result, work was deferred to the manual saw, which saw little to no progress due to the hardness of the material, and finally, to the angle grinder. The angle grinder was capable of cutting through the stainless steel, although the resulting cuts were neither perpendicular nor consistent, compromising the compatibility of the tubing sections. Thus, due to the continued work of cutting, drilling into, and welding the stainless steel, mild-steel tubing was instead ordered and finally delivered on 28 May, delaying the frame assembly by over a week.

7.2.2 10 mm Plate Mismatch

The procured plate for static blades and spacers measured 10 mm in thickness rather than the required 6 mm. This thickness mismatch would have made the static blades physically incompatible with the 6 mm gaps generated by the 6 mm gaps of the rotary spacers. Rather than scrapping and re-ordering the plate, the design was adjusted: all static blades and the spacers would instead be 5 mm thick, with alongside 0.5 mm PETG printed spacers to accommodate

the reduced thickness. While this solution allowed for work to proceed with less delay, several days ere still taken to redesign and re-verify the models.
Altogether, the unexpected stainless frame material and overly thick plate forced the project to pivot from pure manufacturing into alternating cycles of manufacturing and quick CAD redesigns.

7.3 Manufacturing Operations Completed

7.3.1 Plasma-Cutting and Deburring

Using the CNC plasma table in the workshop, the two trainees manufactured all of the following components throughout the two weeks of building:

- Inner panels
- Outer panels
- Flattened sieve
- Static blades
- Rotary blades
- Streel spacers
- Button mount

Immediately after cutting, every part was deburred and, where necessary, hand-finished with files and angle grinders fitted with abrasive discs to ensure that all sufaces were smooth.

7.3.2 Surface Preparation of Cutting Elements

The author and trainees shared the finishing of all holes and slots with rotary tools and files. This work included:

- Spacer centre bores
- Rotary blade centre bores
- Static blade rod bores

The result was the ability to slide each component into either the shaft or rod that it would be fit onto.

7.3.3 Shaft machining

A single 25 mm mild-steel shaft was prepared. An angle grinder flattened a flat section along the full length of the shaft, and final straightness and surface work was completed on a belt sander.

7.3.4 Frame Welding

Once mild-steel tubing arrived, the lowest rectangular layer of the frame (five horizontal struts) were drilled into using Tek self-drilling screws to form M5 threads where future brackets would be bolted on, squared at right angles, alongside a central horizontal strut, and fully welded on all exterior connections. At this stage, only the bottom layer is structurally complete; uprights and upper-level horizontal framing remain unwelded.

7.4 Manufacturing Operations Still Outstanding

Despite the progress detailed in section 7.3, several critical manufacturing and integration work remains incomplete at the time of submission:

- **Frame Fabrication:** Only the lowest rectangular layer has been welded. All vertical struts and upper-level horizontals still need to be tacked, checked for right angles, fully welded, and ground. Until those joints are finished, work cannot proceed on bolting the components and panels to the frame.
- **Bolt Drilling:** The struts that have not part of the base layer have not been drilled and tapped into. As these bolt holes provide an attachment point for all attachments to the frame, such as brackets, work cannot proceed on assembling the components or panels of the shredder together.
- **Mechanical Assembly:** While the shaft blade stack and static blade stack have been assembled as standalone contraptions, they cannot be installed onto the frame due to the incomplete work described above.

Consequently, the shredding mechanism cannot be test-fitted, aligned, or spun.

- **Wiring and Controls:** The ESP32 enclosure, reed sensor, and rotary encoder have not been mounted yet. Wiring still requires routing, crimping, labelling, and connecting, so no electrical commissioning or safety checks can begin.
- **Motor Integration:** The motor base must be fixed to the frame, the coupling height set, the motor height adjusted, and the jaw-type coupler's set-screws fixed. Until then, the shredder cannot be powered.
- **Firmware and Testing:** Control firmware needs to be written, uploaded, debugged, tuned, and verified. A no-load spin test, a PLA shred test, and an emergency-stop test are all pending. Performance data and safety metrics thus remain unavailable.

Until these tasks are completed, the prototype stays in a partial mechanical state and unpowered, leaving functional evaluation impossible.

7.5 On-The-Fly Design Adjustments

The unexpected procurement of 10 mm plate and the delay in mild-steel tubing forced a series of quick CAD revisions that ran concurrently with shop work. First, the 6 mm steel spacers originally specified for the shaft stack were abandoned. Instead, all steel spacers were redrawn at 5 mm and paired with 1 mm PETG spacers printed on the laboratory's 3D printers. This ensured that the total spacing was 6 mm while making future fine-tuning as simple as adding or removing the printed rings. Since static blades must slide be positioned between the rotary blades, both the wide and narrow profiles were also standardised at 5 mm thicknesses, and another set of 3D printed 0.5 mm spacers were placed between rings. This preserved the critical 0.5 mm clearance on each side of every static blade.

Second, the availability of pushbuttons and the emergency stop button at the university laboratory drove the redesign of the button mount. The Schneider Harmony buttons required roughly 35 mm of rear clearance; significantly more than the 30 mm frame depth allowed. Thus, a new button box was therefore

created in SolidWorks using the Sheet-Metal and Edge Flange workflow: a 1 mm aluminium faceplate now creates a box that extrudes from the front outer panel of the shredder, which is bolted on and allows for the mounting of the buttons, providing the switches with the space required. The panel that the button box is mounted on also required plasma cutting under where the box would be mounted in order to provide the space for the buttons.
Third, the ESP32 electronics enclosure had to be reprinted after its original press-fit clips snapped during support-removal. The updated model thickened each clip arm and added triangular ribs at the base to provide rear stress support.
These iterative changes required several redesign sessions between 16 and 25 May but allowed the build to continue with the exception of the frame and frame-assembly themselves.

7.6 Tool Failures and Workarounds

Progress in the workshop was repeatedly interrupted by tool failures over the first two days of work, each one forcing improvised solutions and further contributing to schedule slip.

7.6.1 Industrial Bandsaw (Huvema BMSY 325C)

During the very first stainless-steel cuts, the saw blade overheated and dulled. When the up-feed button was pressed, the dull blade slipped on the wheels and dropped several millimetres, making further use impossible until a replacement blade could be fitted. Work on the frame using the industrial bandsaw was thus stopped and shifted to smaller equipment.

7.6.2 Table-Top Bandsaw

A lighter bench-top bandsaw was used as a replacement for the industrial bandsaw, albeit with cooldown breaks and light pressure application. However, the blade only survived four or five cuts before its teeth suffered the same fate.

At this point, no similar blades remained in the lab aside from manual hack-saws, which took significant effort and consumed far too much time for a single cut of the frame tubing.

7.6.3 Angle-Grinder Cuts

With both saws out of action, frame parts were cut free-hand using an angle grinder. Accuracy deteriorated to approximately ± 3 mm in length and as much as five degrees in squareness.

7.6.4 CNC Plasma-Cutter Crash Sensor

Partway through panel cutting, the machine tripped its safety sensor due to a persistent torch-collision alarm that could not be cleared by normal reset, de-spite no visual indication of a crash having occurred either on the torch head itself nor in the drivetrain. The laboratory supervisor located and fixed the crash sensor trip during the next workday, and cutting resumed with no loss in part accuracy.

7.7 Team Roles and Supervision

The workshop effort was carried out by a three-person team: the author acting as project lead and two second-year mechanical-engineering trainees, **Joonas Ekberg** and **Helmi Nyrökorpi**.

- Author (Project Lead)
    - Sole authority for CAD revisions and all process decisions
    - Performed every welding operation completed to date and all frame drilling with Tek self-tapping screws
    - Marked locations and angles of all cuts
    - Provided continuous safety oversight, foreman work, and real-time guidance
- Trainees

    - Took full responsibility for 100% of the plasma-cutting workload, producing every panel, blade, spacer ring, and sheet-metal bracket
    - Shared deburring, filing, and Dremel work with the author; when normalised for hours (trainees 09:00 – 15:00, author full day) processing effort was roughly equal
    - Bent the angled sieve and the button-mount box using the press
- Supervision Style
    - The author remained physically present throughout most of the trainees' shifts but only intervened when clarification was requested. Both trainees demonstrated competent shop technique and required minimal correction

Across the two weeks, the division of labour allowed design iterations to proceed in parallel with routine processing work, maximizing the limited build window even though key assembly stages could not be reached before the deadline.

8 TESTING AND RESULTS

8.1 Planned Testing

The shredder prototype was scheduled to undergo four baseline trials, each aimed at demonstrating fundamental operation capabilities rather than gathering detailed performance statistics.

8.1.1 No-Load Spin Test

Once the frame was fully welded and the drivetrain installed, the motor would be powered through the VFD and run at nominal RPM with an empty cutting chamber. The objective was to confirm that the shaft blade stack rotated freely,

that bearing alignment was adequate, and that no excessive vibration or mechanical noise indicated mis-machined parts.

8.1.2 PLA Shred Test

After a successful no-load spin, a small PLA printed cube, roughly 30 mm in diameter, would be hand-fed into the hopper. Visual inspection of the output would verify that the machine produced flakes where the majority would be no larger than 5 mm across, thus sufficient for later re-extrusion.

8.1.3 Emergency-Stop Validation

With the machine running under no-load or light-load conditions, the operator would hit the emergency stop button. A successful test would require an immediate cut to motor power and a rapid deceleration of the motor with no more rotation after a few seconds. Passing this check would confirm the correct wiring of the NC contact loop and prepare for the safety interlock shutdown system.

8.1.4 Safety Interlock Test

With the emergency button shutdown sequence being tested and validated, the operator would then test the safety interlock system. The lid would have been opened during operation of the shredder machine. A successful test would entail the shredder immediately ceasing operation and the rapid deceleration of the rotation within a few seconds, similarly to the emergency-stop validation. The success of this test would confirm the accurate wiring and programming of the interlock system.

8.1.5 Planned Testing Conclusions

All four trials were to be carried out using standard laboratory equipment only, with no special fixtures, sensors, or data-logging rigs, so that basic functionality

could be demonstrated quickly before more advanced measures were planned.

8.2 Preliminary Observations

Although none of the planned powered trials could be performed before the deadline, several informal checks conducted during fabrication provided early evidence that key components were fit for operation:

- **Hand-rotation of the blade stack:** After the rotary blades, steel spacers, and PETG spacers were assembled on the shaft, the stack was spun by hand. Rotation was smooth and free of binding, indicating that plasma-cut bores were concentric and that the PETG spacers introduced no measurable wobbling.
- **Fit of static blades and spacers:** The redesigned 5mm static blades, separated by 0.5 mm printed spacers, slid easily into the 6mm gaps between rotary blades without scratching or tilting. The visual clearance confirmed that the new blade thickness and spacers corrected the alignment problems introduced by reducing the static blade thickness.
- **Edge quality of plasma-cut parts:** After deburring, all panel edges, blade perimeters, and bolt holes were visually inspected for finger-safety and edge-accuracy. No significant inaccuracies in the outer edges of plasma-cut materials were observed.

These observations do not replace formal testing, but they do suggest that major alignment and clearance risks identified during redesign were successfully mitigated before full assembly.

8.3 Barriers to Execution

Several compounding obstacles prevented the planned test program from being carried out before the thesis deadline:

- **Material Delays:** The stainless-steel tubing initially acquired proved to be unworkable; correct mild-steel tubing did not arrive until 28 May,

leaving insufficient time to weld the full frame and mount drivetrain components.

- **Tool Failures:** Both the industrial bandsaw and a tabletop bandsaw dulled within a handful of stainless-steel cuts, forcing reliance on an angle-grinder. The resulting inaccuracy required extra grinding time and length incompatibilities, further confirming the need for mild-steel tubing.
- **Redesign Time:** Discovery of 10 mm plate in place of the specified 6 mm triggered a multi-day CAD revision: spacers were redrawn at 56mm, 0.5 mm PETG shims were introduced, and static blades standardized to 5 mm. Further adjustments to the button box and electronics box added more design hours.
- **Print Erros**: A third batch of 3D prints returned with critical parts missing and non-critical parts over-produced (i.e. 20+ copies of a hopper bracket rather than two). Sorting and re-queueing jobs would have consumed another full day of printing and contributed to the decision to end the build-phase ahead of the deadline.
- **Incomplete wiring and motor coupling:** Without the upper frame welded and panels mounted, it was impossible to install the VFD, route conductors, or fix the motor to the shredder. As a result, no powered rotation could be attempted.

Collectively, these setbacks caused the build to be unable to be energised or loaded, making formal testing impossible before the deadline.

8.4 Risks and Future Testing

8.4.1 Outstanding Risks

Until powered trials are completed, several uncertainties remain:

1. **Blade-stack alignment under load:** While hand-rotation was smooth, torque from the motor could amplify any residual axial play or spacer compression, leading to rubbing or jamming.

2. **Motor current draw and thermal rise:** The VFD has yet to be configured and monitored; over-current or overheating could occur if feed-rate is exceeded.
3. **Frame Vibration:** No measurements of oscillation could be taken; excessive vibration could loosen fasteners, damage bearings, or break welds apart.
4. **Emergency-stop reliability:** Wiring, time, and firmware handling of the E-stop remain unverified.
5. **Printed Spacer Durability:** PETG spacers have not been compression-tested; prolonged loading might cause loss of clearance or even melting if shredder shaft temperatures exceed expectations.

8.4.2 Future Test Plan

The following testing is proposed to close the above risks once assembly is completed:

1. **Mechanical Completeness Check:** Tighten all frame bolts, verify bearing load, and re-measure blae-stack clearances.
2. **Electrical Validation:** Test all control and main circuits; configure VFD with ramp-up and current limits; verify E-stop wiring with a multimeter.
3. **No-Load Spin:** Energise motor, log VFD current, and record vibrations.
4. **PLA Shred Test:** Feed a small PLA cube, measure flake size, and confirm no blade rubbing or current spikes.
5. **Incremental Load Testing:** Increase feed rate and material thickness, monitoring motor current and temperatures.
6. **Full-Load Endurance Test**: Operate the shredder continuously for 10 minutes printer scrap. Record VFD current, temperatures, and take note of any audible or visual signs of misalignment.
7. **Emergency-Stop Test:** While running under a full load, trigger the E-stop. Measure stop time with a stopwatch.
8. **Post-Test Inspection:** Remove shaft stack, measure PETG thicknesses at three points each, check for any deformation, and inspect

static-blade edges for burrs and molten plastic, and verify wall-panel bolt tightness.

If all of the above checks pass without abnormal current draw, overheating, excessive vibration, or deformation, the machine can be certified for extended operation and more detailed performance studies can be taken in future works.

9 DISCUSSION

9.1 Recap of Objectives & Key Results

The thesis set out to design, model, prototype, and test a laboratory-scale PLA shredder that advances circular-economy practice inside the university laboratories. Three specific design principles were defined:

1. **Maintainability:** All wear parts must be easy to reach, inexpensive to replace, and where possible, manufacturable in house.
2. **Operational Efficiency:** The shredder should handle the laboratories' filament waste stream with minimal manual intervention or downtime.
3. **Closed-Loop Economy:** Output flakes must be clean and small enough (≤5 mm) to feed directly into the re-extrusion equipment, enabling repeated recycling cycles on campus.

Progress at the submission date is as follows:

- The design and modelling are complete. A full parametric CAD model incorporates easily replaceable components and quick-access bolted panels for simple servicing.
- Prototype fabrication is roughly 40% complete: all plasma-cut components are finished, the blade stacks fit, and the shaft stack rotates freely, and the base frame is fully welded.
- Testing could not be conducted before the deadline due to the remaining incomplete tasks; therefore, no empirical efficiency data or flake-size metrics are available.

While the final commissioning step is still pending, the core maintainability features are already maintained with the parts at hand, and the design now requires only assembly work to reach full operational trials, and no further conceptual changes.

9.2 Critical Reflection on Design and Modelling Choices

9.2.1 Blade-Stack Geometry and Shaft Layout

The alternating sequence of 5 mm rotary blades, 5 mm steel spacers, and 0.5 mm PETG spacers proved to be a robust method of re-aligning the blade stack given the changed standard spacer thickness. The hand-rotation test confirmed that the printed spacers introduced no measurable wobbliness, validating the decision to treat the clearance along the shaft as a simpler design rather than hard-machining the tolerance. The downside is long-term durability: PETG was chosen for its ease of printing and higher glass-transition temperature than PLA, however this temperature may be close to the worst-case temperatures that the shredder may reach. Further iterations may require either nylon or 0.5 mm steel spacers to guarantee long-term stability.

9.2.2 Frame and Panel Strategy

The first batch of frame stock was stainless-steel tubing. Initial cuts on the industrial bandsaw revealed rapid blade dulling, glowing edges, and heavy smoke. Rather than spend more tooling time on a material that the workshop was neither equipped to handle nor would handle it with a sufficient level of precision and accuracy, the decision to abandon stainless steel was made in favour of 30 x 30 x 3 mm mild-steel square tubing.

When the new tubing arrived, each length was mitre-cut at 45 degrees, so that two adjoining members shared a single saw pass, minimising waste and simplifying corner-fits. This approach preserved total tubing length, which allowed for more steel tubing to be used in the case of needing to re-manufacture a frame member which, due to infrequent cutting errors, occurred. The base

rectangle was fully seam-welded; however, no diagonal measurement was taken due to time constraints, so frame squareness remains to be confirmed; especially once the vertical frame struts are added.
Although mitre cuts introduce stricter angle tolerance than square-butt joints, the decision paid off in reduced grinding and a cleaner and sturdier outer profile. Future layers will follow the same 45-degree strategy, provided that cut accuracy can be maintained.

9.2.3 Sheet Metal Modelling

The decision to form the control-panel housing with SolidWorks Edge Flange features rather than fabricating a multi-piece box proved efficient, as it provided a virtual analogue to the real-world fabrication workflow. A single 1 mm sheet can be laser-cut flat, bent on the press, and mounted with ease, giving the pushbuttons the 35 mm of rear clearance required. Due to the author's early lack of knowledge in SolidWorks, this workflow was not enacted for the sieve; a part with similarly bent angles. This increased fabrication time due to the need to calculate dimensions accurately for use with the CNC plasma cutter and forced the estimation of bend locations and angles, rather than having a specific model that served as an analogue to real fabrication. In hindsight, the modelling and fabrication of such pieces of sheet metal could have been optimized by using the sheet metal workflow available in SolidWorks.

9.2.4 Frame Weldments

Similarly to the sheet metal workflow, the author was also unaware of the SolidWorks weldments feature at the time of modelling the shredder frame. The frame therefore consists of basic hollow-square extrusions positioned manually, with each length manually entered and no parameterised mitre angles or internal labelling for frame members inside the CAD file. This choice carried several key penalties:

1. **Missing automatic cut-list:** Since the model was not a weldment, SolidWorks could not generate a standard cut-list table. Every tube

length thus had to be manually extracted and copied into a spreadsheet and marked on the physical members once cut. When stainless steel was abandoned and mild-steel tubing arrived, every dimension had to be verified by hand. The cut-list tool would have optimized this process and saved time in cutting and welding preparations.

2. **Higher risk of misidentification:** A manual face-level-orientation labelling system was invented and written on the tubes after cutting. Had weldments been used, each member would have carried a unique, automatic identifier, further simplifying and optimizing the workflow, and preventing material waste due to mislabelling and misidentifying frame members.

Rebuilding the frame as a weldment part would have automated the process of decision-making for cutting the frame apart in several ways including providing an automatic cut-list and automatically labelling the frame members correctly to avoid later misidentification errors.

9.3 Manufacturing Experience and Team Dynamics

9.3.1 Timeline Slippage

The build began on 14 May with an optimistic schedule. Two unforeseen factors drove most of the delay: material mismatches and tool failures. The switch from stainless to mild-steel tubbing added more than a week of waiting, and both the industrial and tabletop bandsaws failed early before the switch, forcing labour-intensive angle-grinder cuts. In parallel, the arrival of 10 mm plate triggered a redesign cycle that consumed the entire weekend of 17-18 May. By the time the correct materials reached the lab (28 May), only two days of fabrication time remained; insufficient for welding, wiring, and testing.

9.3.2 Collaboration with Trainees

Second-year mechanical engineer students Joonas Ekberg and Helmi Nyrökorpi handled every plasma-cutting job and half of all deburring and filing

hours. Their fixed 09:00 – 15:00 schedule, combined with the author's full-day workdays, produced an approximately equal share of processing effort after normalising for hours. Supervision was largely hands-off: DXF files and a brief daily briefing were enough or the trainees to work autonomously, freeing the author to focus on redesigns, and at the later stages, welding.

9.3.3 Laboratory Resource Availability

Since the build coincided with the university's summer break, virtually all major shop equipment was idle. The CNC plasma table, press, and grinders were available on demand, so international competition for machine time played no role in the schedule slip. The only temporary limitation was the dulled blade on the industrial bandsaw, and a replacement had to be ordered. However, the issue became moot once stainless-steel tubing was abandoned during the first two days. When mild-steel tubing arrived, a fresh blade was already installed and cutting proceeded without interruption.

A separate complication arose when the third batch of 3D prints returned with an unexpected mix of parts: dozens of hopper brackets were produced while the required panel brackets were missing. The mismatch appears to have occurred somewhere between the job ticket and printer queue. Although the error did not halt progress as the frame was still awaiting welding, it underscored the value of verifying print-queue outputs before committing to large part runs.

9.4 Technical Limitations of the Prototype

The partially assembled shredder exhibits several unresolved limitations that must be addressed before it can be relied on for routine laboratory use:

- **Structural Uncertainty:** Only the base frame rectangle is fully welded; the vertical and upper horizontal frame are still not welded. Until those joints are welded, overall frame stiffness and bearing alignment remain unknown.
- **Dimensional Inaccuracy in Cut Struts:** Angle-grinder cuts on the stainless-steel tubing showed length errors of up to ± 3 mm and skew

angles of about 5 degrees. Although the mild-steel members were mitre-cut on a bandsaw, no final trim or diagonal check has been undertaken aside from the visual inspection and welding of the base layer. Any residual mis-cuts will translate into misalignments once the upper layers are welded.

- **Unverified Blade Stack Clearance:** The redesigned 5 mm static blades and PETG spacers fit correctly by hand, but their clearance under motor torque due to thermal expansion remains untested. During extended runs, this clearance may decrease.
- **Undocumented Vibration:** No vibration testing has been undertaken. Excessive vibration could loosen panels and bolts and cause the part wear during extended runs.
- **Flake Size Uncertainty:** While the theoretical framework for achieving the expected flake size is valid, it remains to be seen if the true output of the shredder will result in consistent flakes sized at or under 5 mm.

Collectively, these gaps mean the prototype cannot yet validate its core claims of operational efficiency or closed-loop recyclability. Subsequent work must close each limitation before the shredder can be adopted in routine laboratory workflows.

9.5 Sustainability & Circular-Economy Implications

Although the shredder is not yet operational, its design already supports key circular-economy principles adopted by the university laboratories:

- **Local Recycling Loop:** The machine is sized to handle the filament waste and failed prints generated in the automation lab. If the machine is used at even half-capacity once completed, the labs could reuse a significant volume of filament waste every year, reducing both landfill and virgin filament purchases.
- **In-House Manufacturing and Repair:** All critical wear parts (rotary blades, static blades, spacers, etc…) can be reproduced using existing plasma-cutting and 3D printing equipment. This aligns with

maintainability objectives and minimises transport-related emissions associated with spare-part procurement.

- **Material Utilisation:** Mitre-cut frame joints and the single-sheet button box and sieve were chosen for ease of manufacturing and for limiting scrap. The shift to 5 mm plates and printed spacers further reduced waste by eliminating the need to source a second thickness.
- **Component Waste Recycling:** Due to the nature of all brackets being printed in PLA, aside from the rod bearings for the static blade stack, any waste generated by these materials can be recycled in the shredder once completed, and any spare brackets can similarly be recycled.

In summary, the prototypes architecture is already consistent with the university's circular-economy goals. Competing the remaining assembly and verification steps will convert these benefits to measurable environmental savings.

9.6 Risk Assessment & Mitigation Strategies

A preliminary hazard analysis was carried out to identify the most significant risks remaining in the partly built shredder and to outline practical countermeasures that should be implemented before commissioning.

9.6.1 Mechanical Risks

Dull edges can force higher torques, and due to the nature of the blade cutting edges being dull, this additional torque may cause increased wear on load-bearing components. Furthermore, slight axial drift along the blade stacks could lead to contact between the blade stacks. To mitigate this risk, a verification procedure could be maintained at specified intervals (i.e. every 20kg of PLA shredded) to re-verify spacer compression and alignment.

Unfinished welds and uneven sizing may cause certain frame members to bear unequal loads, where they would theoretically bear identical loads. Thus, to mitigate this risk, all welds must be completed, ground flat, and frame squareness must be confirmed before installing the shaft. Furthermore, during servicing, the frame must be inspected for bending and stress-induced wear.

9.6.2 Electrical Control Risks

The stop and E-stop buttons remain to be wired to the VFD’s safety inputs. To mitigate the risk of failure in the emergency system, continuity tests must be performed on all NC circuits, and the addition of a secondary safety relay for redundancy can be considered.

9.6.3 Risk Conclusion

By addressing these hazards systematically and incorporating sturdy safety checks and inspections, the shredder can safely move from prototype status to routine laboratory equipment. Further risk analysis can be conducted once the basic operations and safety procedures are verified and validated and will contribute to a more resilient and robust machine.

10 CONCLUSION

This thesis set out to design, model, and begin prototyping a laboratory-scale shredder that would enable the university’s laboratories to recycle their own PLA waste, thus closing the material loop and supporting circular-economy goals. The work produced a fully parametric CAD model; complete sets of plasma-cut panels, blades, and spacers; frame members and a partially welded frame; and an electronics system that emphasises maintainability and local manufacturability. Although shortages and tool failures prevented final assembly and powered testing, the core engineering challenges of blade geometry, shaft alignment, tolerance management, and frame layout, have been solved in a way that can now be replicated with minimal further conceptual change.

Several practical lessons have been learned. Firstly, modelling sheet-metal parts and mitred frames directly in SolidWorks’ sheet metal and weldments

workflows would have significantly aided in production time and optimized both efforts and time-management. Secondly, the printed spacers proved an effective stopgap for fine axial alignment, demonstrating that additive manufacturing can replace precision machining in early prototypes, provided that long term wear-and-tear is monitored. Third, delegating plasma cutting and routine finishing tasks to well-briefed trainees freed design capacity, proving that well-thought-out delegation of tasks and efforts supports project efforts significantly. Fourth, the material acquisition errors proved the necessity of strict definitions for required materials and similarly strict acquisition efforts in order to ensure that further processes proceed as expected.

To transform the present sub-assembly into a functioning shredder, four immediate actions are required:

1. Complete welding of the upper frame layers and drill all bolt holes.
2. Mount bearings, shaft, blade stack, and sieve, confirming 0.5 mm clearances.
3. Install and configure the VFD and program the shredder's logic.
4. Run the planned no-load spin, PLA shredding test, safety trials, and log current draw and vibrations.

Longer-term work should focus on endurance testing of PETG spacers, refinement of inspection intervals, and integration with the laboratory's filament re-extrusion line. Once those steps are completed, the prototype promises to divert a significant volume of PLA waste each year from the landfill while reducing the labs' demand for virgin filament. The project therefore provides a concrete path towards an in-house circular-economy ecosystem and a practical learning platform for future students in sustainable design and manufacturing.

REFERENCES

ams-OSRAM. (2025). *Presence and speed detection with dToF Presence and speed detection with dToF Presence and speed detection with dToF Valid for: TMF8X0X, TMF882X*. https://ams-osram.com/https://ams-osram.com/https://ams-os-

Ancha, S., Cmu, K. F., Burgard, W., & Nuremberg, T. U. (2022). *Active Robot Perception using Programmable Light Curtains*.

European Commission. (2020). *Circular economy action plan*. https://environment.ec.europa.eu/strategy/circular-economy-action-plan_en

Hafiz, H. M., Al Rashid, A., & Koç, M. (2024). Recent advancements in sustainable production and consumption: Recycling processes and impacts for additive manufacturing. In *Sustainable Chemistry and Pharmacy* (Vol. 42). Elsevier B.V. https://doi.org/10.1016/j.scp.2024.101778

Harjuma, H., Tahir, A., Sirama, S., & Aswar, A. (2024). Development of Plastic Shredder Technology to Support Plastic Waste Reduction. *International Journal of Engineering, Science and Information Technology*, *5*(1), 77–84. https://doi.org/10.52088/ijesty.v5i1.643

Hasan, M. R., Davies, I. J., Pramanik, A., John, M., & Biswas, W. K. (2024). Potential of recycled PLA in 3D printing: A review. *Sustainable Manufacturing and Service Economics*, *3*, 100020. https://doi.org/10.1016/j.smse.2024.100020

Landolfi, L., Detry, A. L. H. S., Cozzolino, E., Tammaro, D., & Squillace, A. (2024). Energy-saving approach for mechanical properties enhancement of recycled PET additively manufactured by MEX. *Sustainable Materials and Technologies*, *41*. https://doi.org/10.1016/j.susmat.2024.e01038

Romani, A., Perusin, L., Ciurnelli, M., & Levi, M. (2024). Characterization of PLA feedstock after multiple recycling processes for large-format material extrusion additive manufacturing. *Materials Today Sustainability*, *25*. https://doi.org/10.1016/j.mtsust.2023.100636

Song, Y., Li, Y., Song, W., Yee, K., Lee, K. Y., & Tagarielli, V. L. (2017). Measurements of the mechanical response of unidirectional 3D-printed PLA.

Materials and Design, *123*, 154–164. https://doi.org/10.1016/j.matdes.2017.03.051

The Next Layer. (2024, March 11). *Affordable Filament Recycling?* [Video recording]. YouTube. https://www.youtube.com/watch?v=Hm6KpEajD4o

Torres, J., Cotelo, J., Karl, J., & Gordon, A. P. (2015). Mechanical property optimization of FDM PLA in shear with multiple objectives. *JOM*, *67*(5), 1183–1193. https://doi.org/10.1007/s11837-015-1367-y

Wong, J. H., Gan, M. J. H., Chua, B. L., Gakim, M., & Siambun, N. J. (2022). Shredder machine for plastic recycling: A review paper. *IOP Conference Series: Materials Science and Engineering*, *1217*(1), 012007. https://doi.org/10.1088/1757-899x/1217/1/012007

Zhu, C., Li, T., Mohideen, M. M., Hu, P., Gupta, R., Ramakrishna, S., & Liu, Y. (2021). Realization of circular economy of 3D printed plastics: A review. In *Polymers* (Vol. 13, Issue 5, pp. 1–16). MDPI AG. https://doi.org/10.3390/polym13050744

LoveJoy. (n.d.). L Type – Standard Jaw Coupling [STEP file]. LoveJoy Inc. https://www.lovejoy-inc.com/products/jaw-type-couplings/l-type-standard-jaw-coupling/

Petkov, T. (2014). Reed switch [STEP file]. GrabCAD Community. https://grabcad.com/library/reed-switch-1?utm_source=chatgpt.com

Shuja, H. (2021). 38 mm OD, 6 mm Shaft, Incremental Optical Rotary Encoder [STEP file]. GrabCAD Community. https://grabcad.com/library/38-mm-od-6-mm-shaft-incremental-optical-rotary-encoder-1?utm_source=chatgpt.com

MP3D. (2024). Push-Button Switch COLOR Ø22 (White-red-green-yellow) [SLDPRT file]. GrabCAD Community. https://grabcad.com/library/push-button-switch-color-o22-white-red-green-yellow-1

Steyn, D. (2022). 22mm Emergency Stop Button [STEP file]. GrabCAD Community. https://grabcad.com/library/22mm-emergency-stop-button-1

Okutan, Ö. (2017). UCP 205 BEARİNG [SLDASM file]. GrabCAD Community. https://grabcad.com/library/ucp-205-bearing-1/details?folder_id=3317723

CNC Kitchen. (2025). Threaded Inserts / Heat Set Inserts by CNC Kitchen [STEP file]. Printables. https://www.printables.com/model/482734-threaded-inserts-heat-set-inserts-by-cnc-kitchen/files

SEW-EURODRIVE. (2025). R77DRN90L4 - R Series Helical Gear Units [STEP file]. SEW-EURODRIVE CAD Configurator.